Copy 7
RM SL50E09a

NACA

RESEARCH MEMORANDUM

for the

Bureau of Ships, Department of the Navy

DATA FROM TESTS OF A $\frac{1}{5}$-SCALE MODEL OF A PROPOSED HIGH-SPEED SUBMARINE IN THE LANGLEY FULL-SCALE TUNNEL

By Bennie W. Cocke, Stanley Lipson, and William I. Scallion

Langley Aeronautical Laboratory
Langley Air Force Base, Va.

NATIONAL ADVISORY COMMITTEE
FOR AERONAUTICS

WASHINGTON

MAY 5 1950

NATIONAL ADVISORY COMMITTEE FOR AERONAUTICS

RESEARCH MEMORANDUM

for the

Bureau of Ships, Department of the Navy

DATA FROM TESTS OF A $\frac{1}{5}$-SCALE MODEL OF A PROPOSED HIGH-SPEED SUBMARINE IN THE LANGLEY FULL-SCALE TUNNEL

By Bennie W. Cocke, Stanley Lipson, and William I. Scallion

INTRODUCTION

Tests of a $\frac{1}{5}$-scale model of a proposed 153-foot high-speed submarine have been conducted in the Langley full-scale tunnel at the request of the Bureau of Ships, Department of the Navy.

The test program included: (1) force tests to determine the drag, control effectiveness, and static stability characteristics for a number of model configurations, both in pitch and in yaw, (2) pressure measurements to determine the boundary-layer conditions and flow characteristics in the region of the propeller, and (3) an investigation of the effects of propeller operation on the model aerodynamic characteristics.

In response to oral requests from the Bureau of Ships representatives that the basic data obtained in these tests be made available to them as rapidly as possible, this data report has been prepared to present some of the more pertinent results. All test results given in the present paper are for the propeller-removed condition and were obtained at a Reynolds number of approximately 22,300,000 based on model length.

SYMBOLS AND COEFFICIENTS

The symbols and coefficients used in the presentation of data were chosen in accordance with one of the standard systems given in reference 1. All moment coefficients presented have been computed about a model center of gravity which corresponds to the full-scale submarine center-of-gravity location specified by the Bureau of Ships as 9.05 feet forward of the midlength point and 13.94 feet above the base line.

D'	drag coefficient $\left(\frac{D}{\frac{1}{2}\rho l^2 U^2}\right)$
Y'	lateral-force coefficient $\left(\frac{Y}{\frac{1}{2}\rho l^2 U^2}\right)$
K'	rolling-moment coefficient $\left(\frac{K}{\frac{1}{2}\rho l^3 U^2}\right)$
M'	pitching-moment coefficient $\left(\frac{M}{\frac{1}{2}\rho l^3 U^2}\right)$
N'	yawing-moment coefficient $\left(\frac{N}{\frac{1}{2}\rho l^3 U^2}\right)$
D	drag force in direction of relative flow, pounds
Y	lateral-force component, positive for force acting to starboard, pounds
K	rolling moment, positive when acting to produce heel to starboard, foot-pounds
M	pitching moment, positive when acting to produce positive pitch (nose up), foot-pounds
N	yawing moment, positive when acting to produce yaw to starboard, foot-pounds
ρ	mass density of air, $\frac{\text{pound-second}^2}{\text{feet}^4}$
U	free-stream velocity, feet per second
l	length of body (30.667 ft)
u	local velocity, feet per second
α	angle of attack, positive nose up, degrees
ψ	angle of yaw, positive nose to starboard, degrees

δ_r — rudder angle, positive when trailing edge deflected to port, degrees

δ_s — stern-plane angle, positive when trailing edge deflected down, degrees

R — Reynolds number $\left(\frac{\rho l U}{\mu}\right)$

P — static-pressure coefficient $\left(\frac{p - p_o}{q_o}\right)$

C_p — dynamic-pressure coefficient $\left(\frac{h - p_o}{q_o}\right)$

p — local static pressure, pounds per square foot

p_o — free-stream static pressure, pounds per square foot

q_o — free-stream dynamic pressure, pounds per square foot $\left(\frac{\rho U^2}{2}\right)$

μ — absolute viscosity of air, pound-seconds per square foot

q — local dynamic pressure, pounds per square foot $\left(\frac{\rho u^2}{2}\right)$

δ_{dr} — bridge fairwater dorsal rudder angle, positive when trailing edge deflected to port, degrees

MODEL

The model used in these tests was 1/5 full scale and was constructed to duplicate as closely as possible the details of double-hull construction such as bulkhead locations, margin-plate installations, and so forth as shown on Bureau of Ships drawings for the full-scale submarine. Flooding and venting hole dimensions for the model were 1/5 scale and the hole arrangements corresponded closely in number and location to those specified for the full-scale submarine.

Photographs of the model for several test configurations are shown in figures 1 to 7.

DATA PRESENTATION

Drag

The results of the drag investigation are summarized in table I and drag polars for three of the configurations are shown in figure 8. These results indicate that the drag of the complete scheme-2 configuration (D' = 0.00188) is 63.4 percent higher than the drag of the basic hull (D' = 0.00115). This drag coefficient increase of 0.00073 is composed of increments of 0.00028 for the rear tail installation (fig. 2), a total of 0.00027 charged to all flooding and venting openings, and 0.00018 for the scheme-2 bridge fairwater (fig. 7). Tests of the minimum bridge fairwater and the forward-located tail installation show that the complete model drag would be reduced approximately 10 percent with these alternate appendages installed. The detailed flow studies in the junctures of the bridge fairwater and the tail assemblies indicated that, except at the sharp afterbody of the minimum bridge fairwater, no separation tendencies were evident. The attempt to reduce the drag of the scheme-2 rear tail configuration by extending the chord and reducing the trailing-edge angle of the thick inboard strut and by filleting the sharp step juncture did not result in any appreciable drag reduction; this result is attributed to the fact that the greater portion of this section of the tail was enveloped by the thick boundary layer of the hull.

Static Stability

Some of the more significant results of the stability investigation are presented in figures 9 to 14. The effect of the three stabilizer and diving-plane configurations on the variation of the pitching-moment coefficient with angle of attack is shown in figure 9 and with diving-plane deflection, in figure 10. Figure 11 presents the pitching-moment coefficient stern-plane deflection curves for $\alpha = -0.3^{\circ}$ from figure 10 as an aid in rapidly comparing the static longitudinal stability of the three diving planes. While the data are not presented herein, test results show the scheme-2 bridge fairwater gives a small nose-up pitching tendency (M', approximately 0.0002) throughout the α range investigated (5.7° to -6.3°).

The variations of yawing-moment coefficient, rolling-moment coefficient, pitching-moment coefficient, and lateral-force coefficient, with angle of yaw, are presented in figure 12 for five different appendage arrangements on the operational hull. The operational hull is defined as the basic body with all vent and flood holes open. The model configurations were selected so that the effects in yaw of the scheme-2 rudder, the forward located rudder, the scheme-2 bridge fairwater, and the minimum bridge fairwater may be separated and analyzed, either alone or for various operational arrangements. The destabilizing effect of the large scheme-2 bridge fairwater on the lateral stability characteristics is very evident in the data presented in figure 12. The relative ineffectiveness of the scheme-2 bridge fairwater dorsal rudder (fig. 7) is shown in figure 13 for two angles of yaw. The effectiveness of the rudder of the forward tail configuration is shown in figure 14 to be greater at the higher deflections than that for the rear scheme-2 tail configurations.

Boundary Layer and Wake Surveys

The results of pressure surveys obtained on the hull surface, in the boundary layer at the aft portion of the hull, and in the body wake, both at the propeller disk and 9 inches behind the model, are presented in figures 15 to 18. The variations with yaw of the surface static pressures measured along the longitudinal center line on the starboard side of the hull are shown in figure 15. The sharp break in the pressure distribution occurring approximately $2\frac{1}{2}$ feet aft of the nose is caused by a slight discontinuity in the hull surface where the nose section, which was readily removable for maintenance purposes, joined the main part of the hull. Figure 16 presents the boundary-layer velocity profiles in fractions of free-stream velocity along the aft portion of the hull. All of the boundary-layer surveys were made along the longitudinal center line of the upper surface of the hull. The wake surveys are shown in figure 17 for the scheme-2 rudder and 332-square-foot diving-plane installation and in figure 18 for the forward tail-surface arrangement. For the former configuration, two survey locations were investigated, one at the propeller disk (fig. 17(a)) and one 9 inches aft of the propeller disk. These results are presented as contour plots showing lines of constant ratios of local dynamic pressure to free-stream dynamic pressure with the measured local static-pressure coefficients indicated throughout the wake.

Langley Aeronautical Laboratory
National Advisory Committee for Aeronautics
Langley Air Force Base, Va.

Bennie W. Cocke Jr

Bennie W. Cocke
Aeronautical Research Scientist

Stanley Lipson

Stanley Lipson
Aeronautical Research Scientist

William I. Scallion

William I. Scallion
Aeronautical Engineer

Approved: Mark R. Nichols
for Clinton H. Dearborn
Chief of Full-Scale Research Division

omm

REFERENCE

1. Landweber, L., and Abkowitz, M. A.: A Proposed Nomenclature for Treating the Motion of a Submerged Body through a Fluid. Rev. ed., Dec. 1948. (Prepared for Committee on Nomenclature of American Towing Tank Conference.)

TABLE I

SUMMARY OF DRAG MEASUREMENTS

Test	Model configuration	D' at α = 0	ΔD'
1	Basic hull. Appendages removed; flood and vent openings sealed and faired	0.00115	--------
2	Same as 1 except scheme-2 fin and rudder installed with the 332-square-foot diving plane and elevator	.00143	0.00028
3	Same as 2 except superstructure flooding and venting holes open aft of bulkhead 32	.00150	.00007
4	Same as 3 except superstructure flooding and venting holes open aft of bulkhead 4	.00161	.00011
5	Same as 4 except all superstructure flooding and venting holes open	.00165	.00004
6	Same as 5 except ballast tank flood holes open aft of bulkhead 32	.00168	.00003
7	Same as 6 except ballast tank flood holes open aft of bulkhead 4	.00168	--------
8	Same as 7 except all ballast tank and venting holes open	.00170	.00002
9	Same as 8 except minimum bridge fairwater installed	.00182	.00012
10	Same as 8 except scheme-2 bridge fairwater installed (Complete scheme-2 configuration)	.00188	.00018
11	Same as 10 except fillets and fairings installed on scheme-2 tail surfaces	.00187	-.00001
12	Same as 10 except rear located scheme-2 control surfaces removed	.00160	-.00028
13	Same as 12 except scheme-2 rear-located fin and rudder installed with the 202-square-foot diving plane and elevator	.00184	.00024
14	Same as 13 except forward-located control surfaces installed	.00177	.00017

NACA

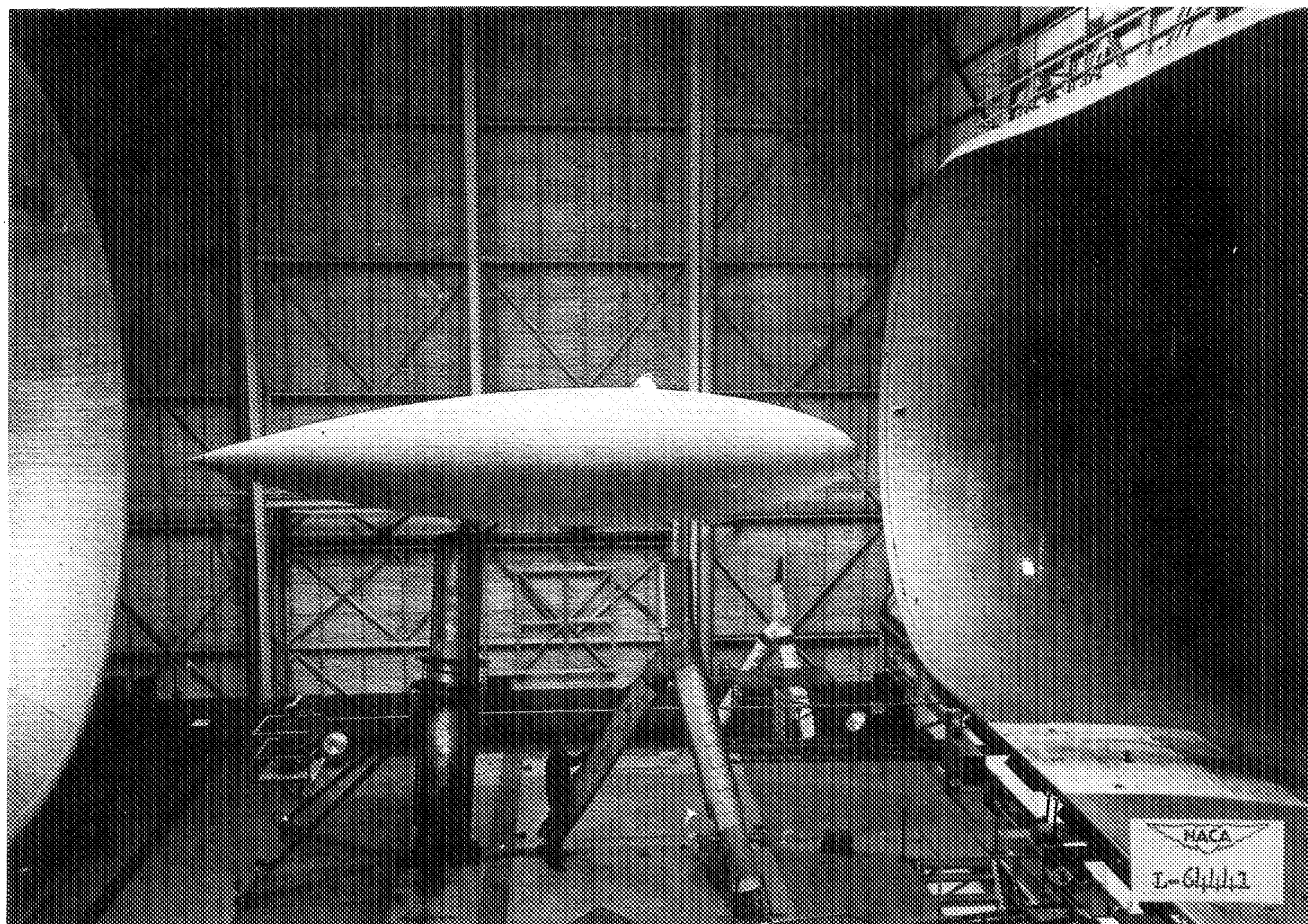

Figure 1.- General view of model in basic hull condition.

CONFIDENTIAL

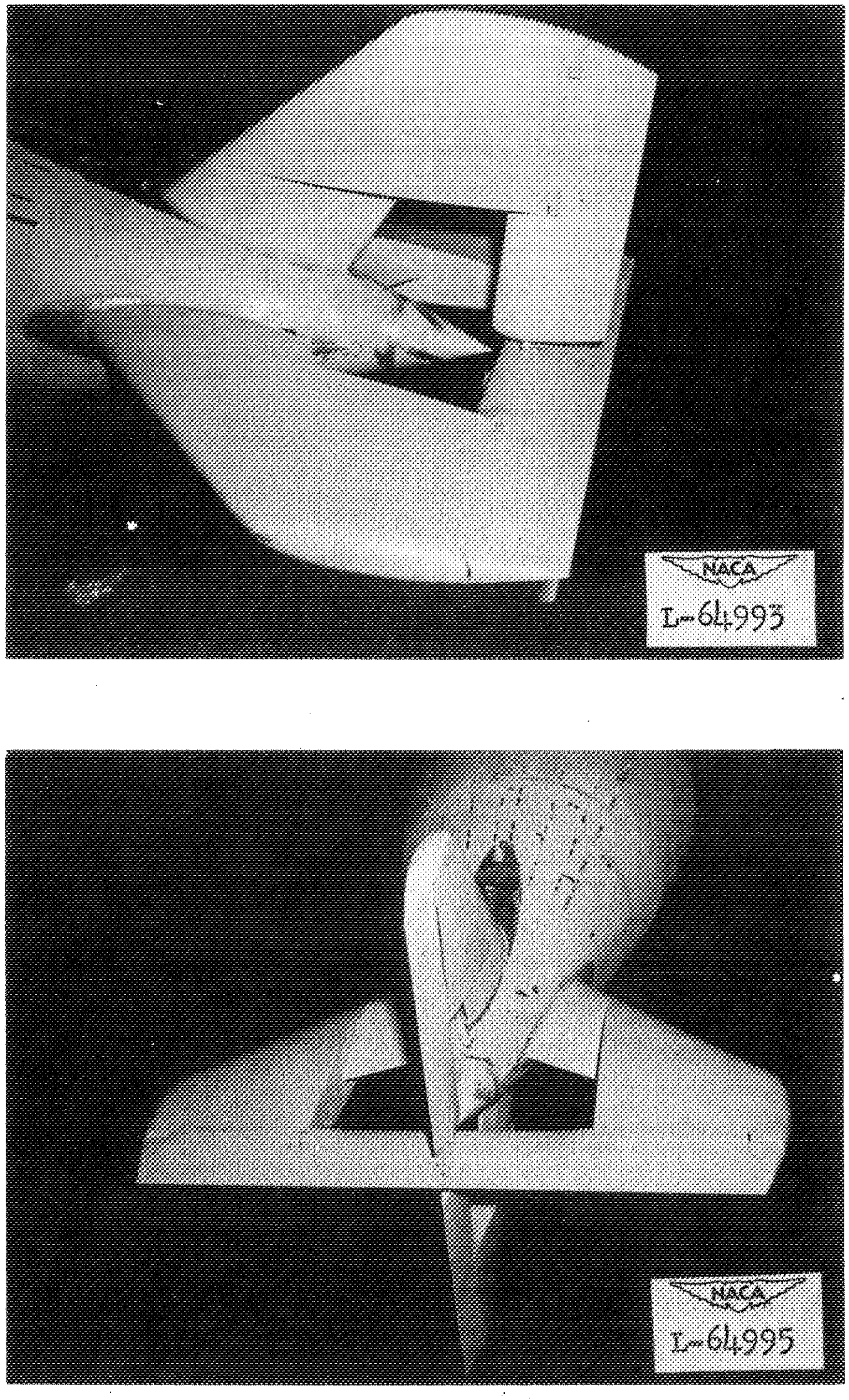

Figure 2.- Scheme-2 fin and rudder with 332-square-foot diving planes installed.

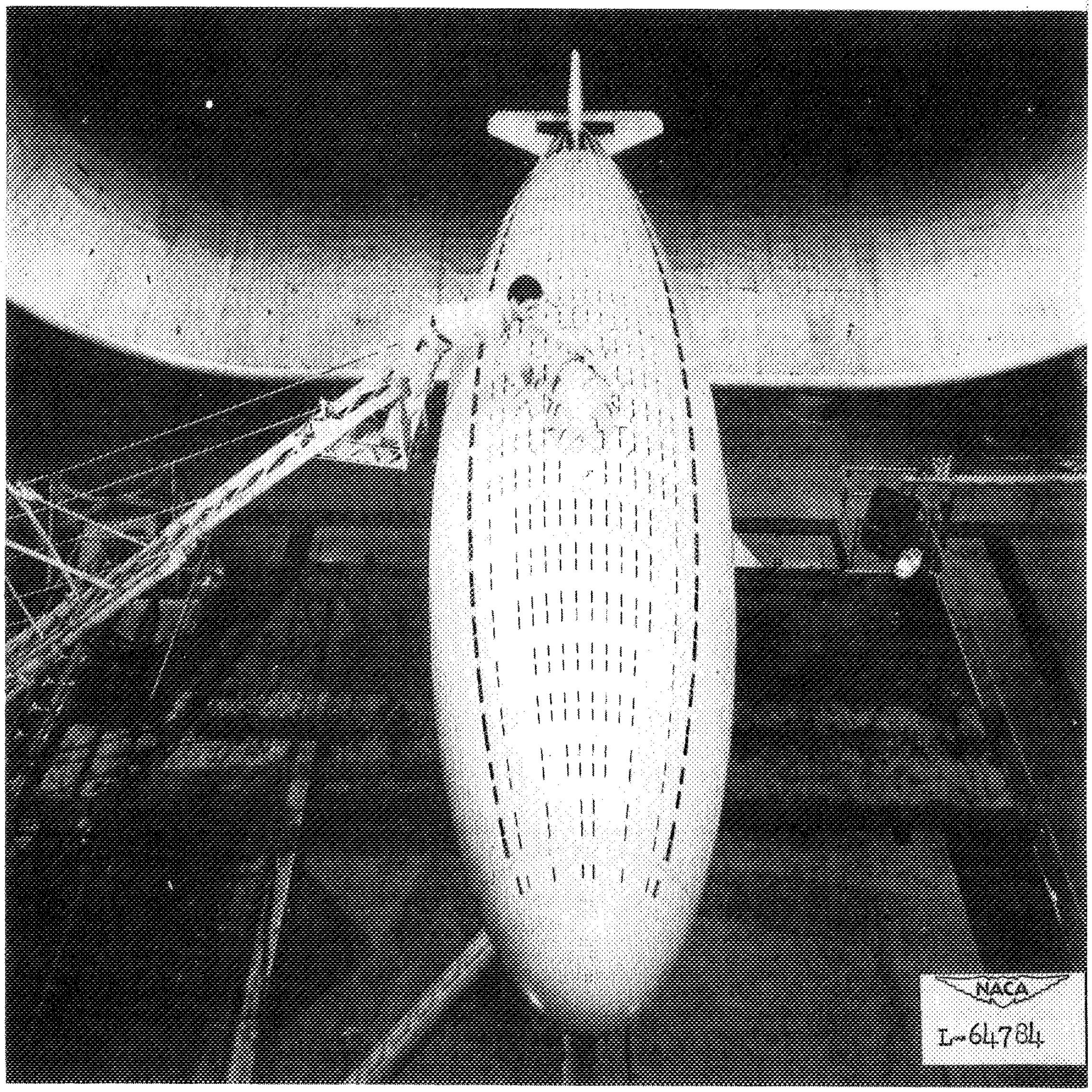

Figure 3.- Superstructure flooding and venting hole arrangement with minimum bridge fairwater installed.

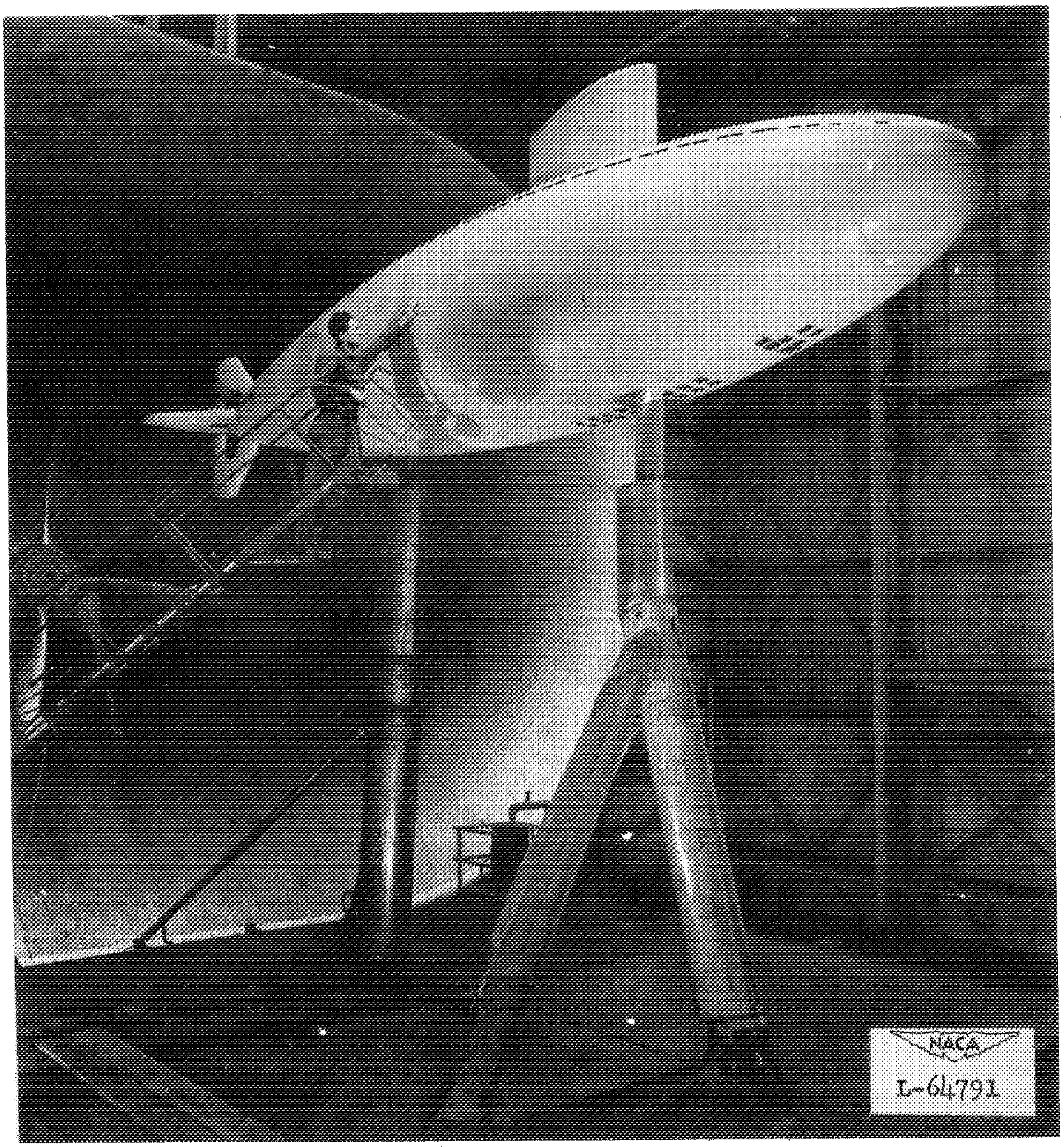

Figure 4.- Main ballast tank flood holes with scheme-2 bridge fairwater installed.

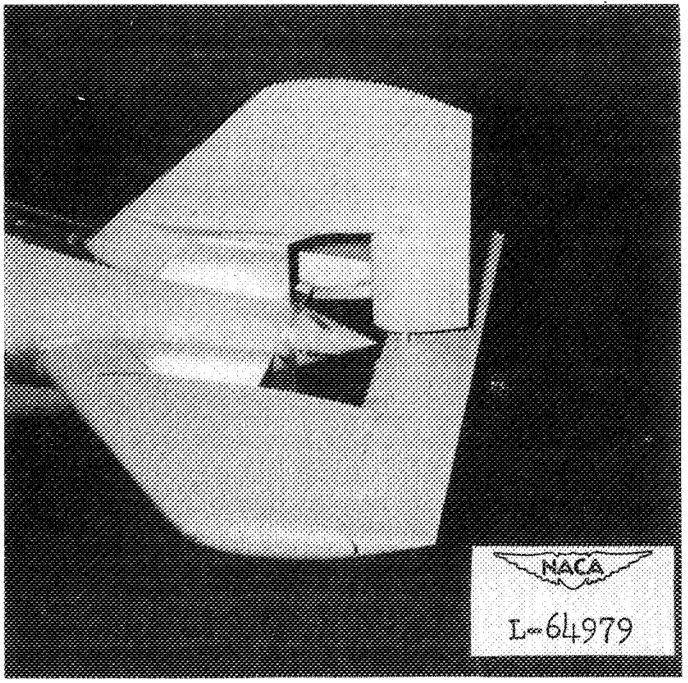

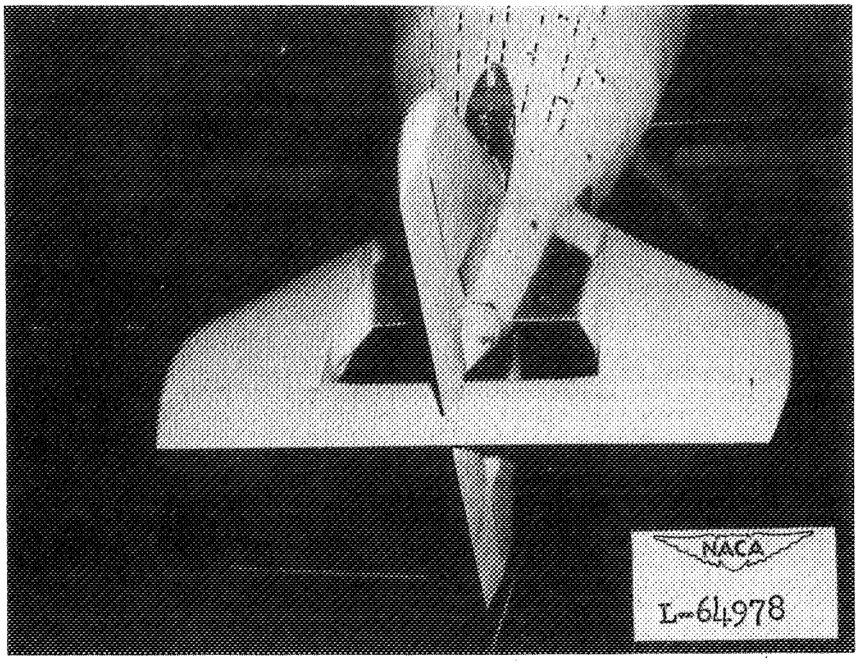

Figure 5.- Modified scheme-2 tail installation.

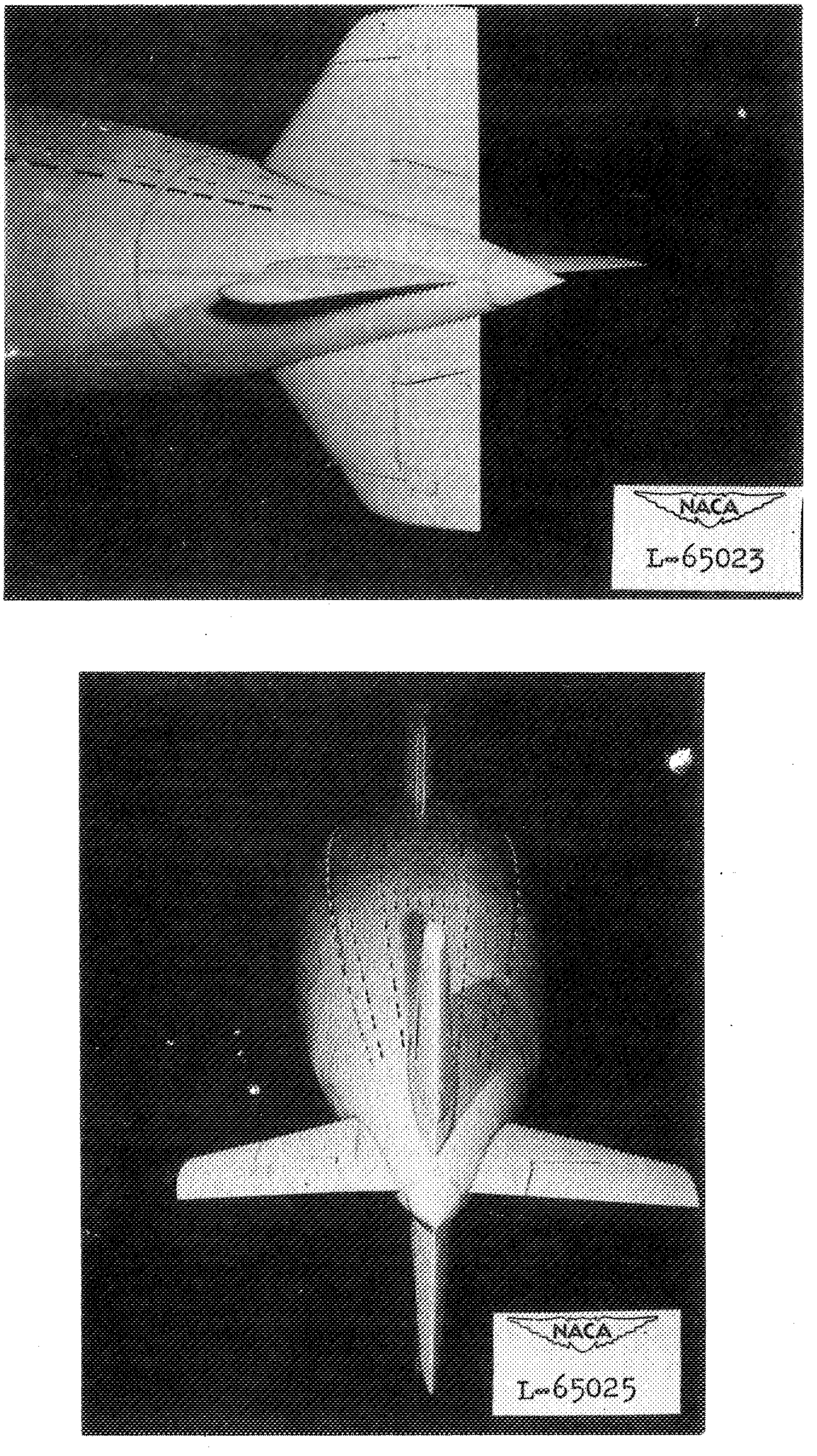

Figure 6.- Forward-located tail-surface arrangement.

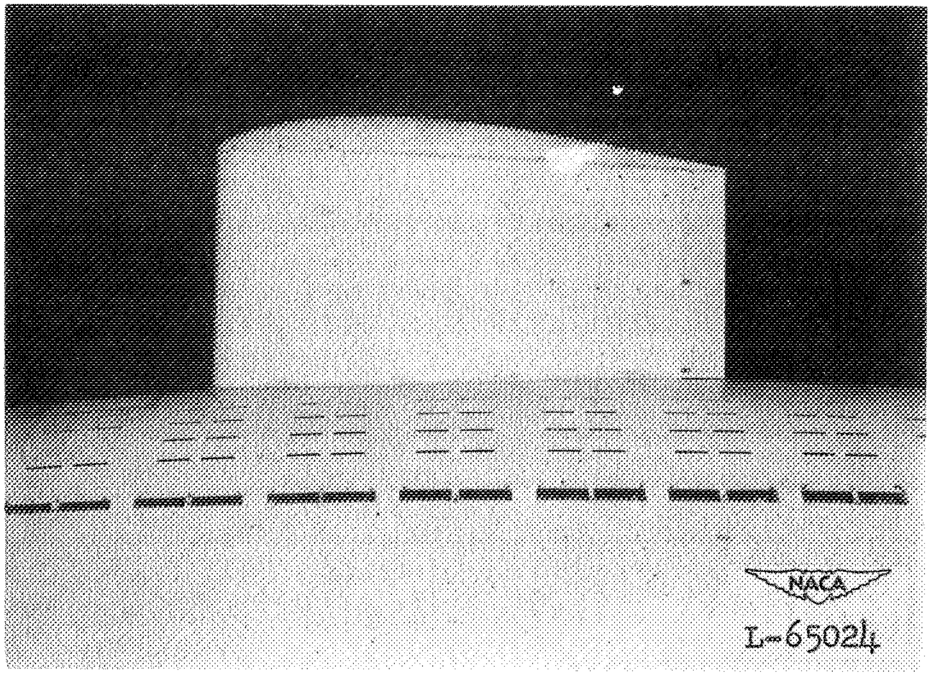

Figure 7.- Scheme-2 bridge fairwater.

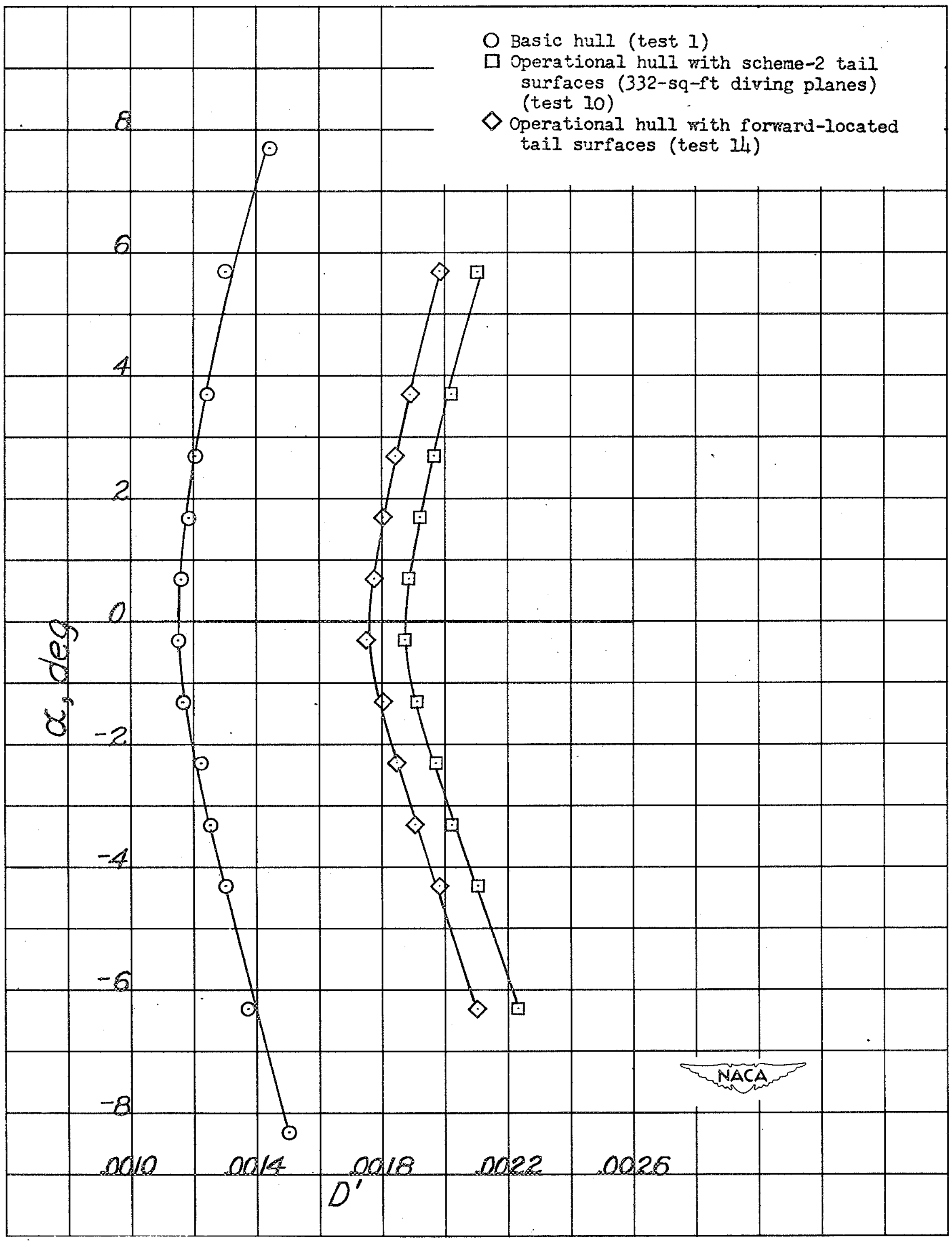

Figure 8.- Variation of drag coefficient with angle of attack for three model configurations. (See table I.) $\psi = 0^{\circ}$; $\delta_r = 0^{\circ}$; $\delta_s = 0^{\circ}$.

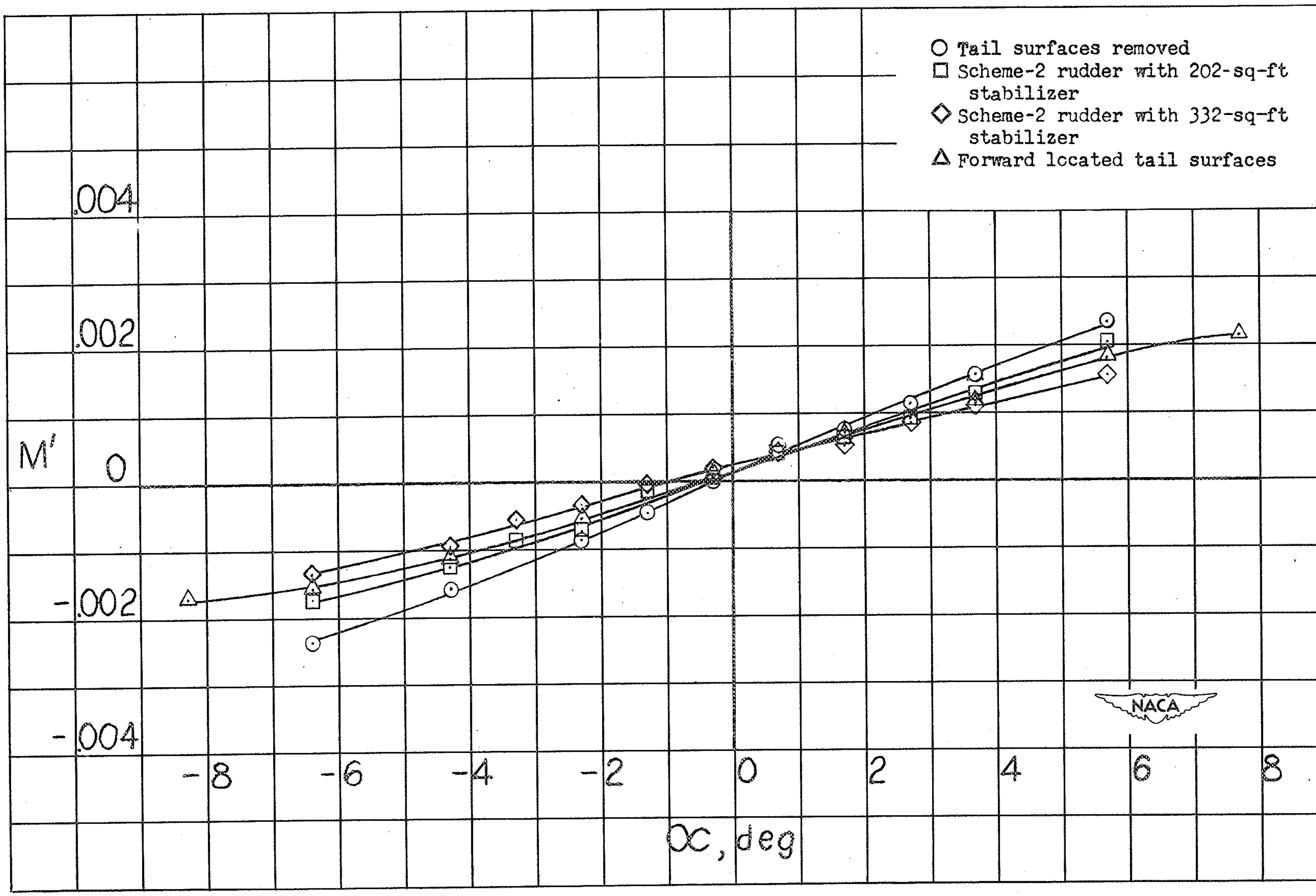

Figure 9.- Variation of pitching-moment coefficient with angle of attack for operational hull, including bridge fairwater, with and without tails installed. $\psi = 0^{\circ}$; $\delta_s = 0^{\circ}$; $\delta_r = 0^{\circ}$.

3161 10

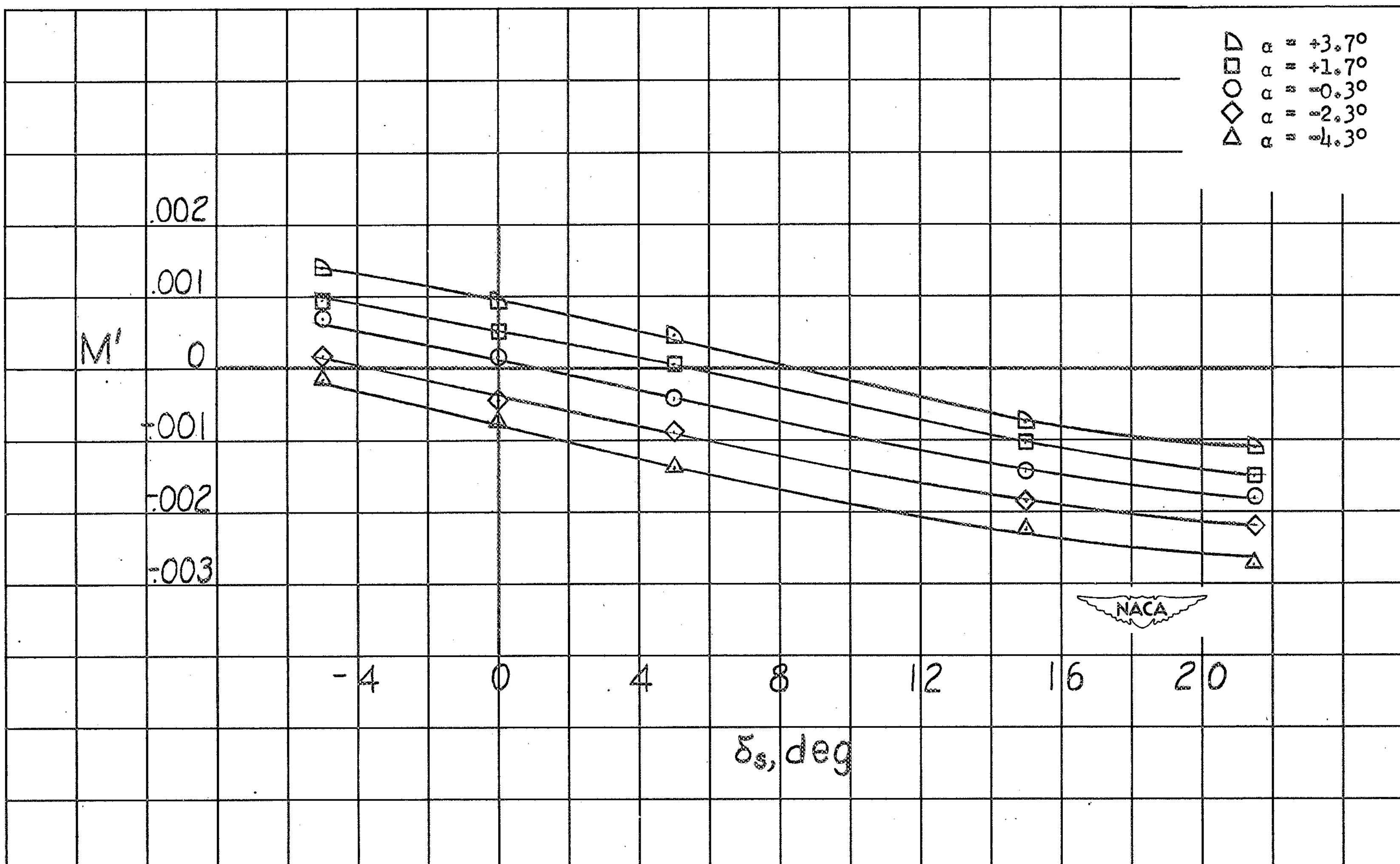

NACA SL50E09a

CONFIDENTIAL

CONFIDENTIAL

(a) Scheme-2 tail with 332-square-foot diving plane.

Figure 10.- Variation of pitching-moment coefficient with diving-plane deflection and α for three tail configurations. $\psi = 0^{\circ}$; $\delta_r = 0^{\circ}$.

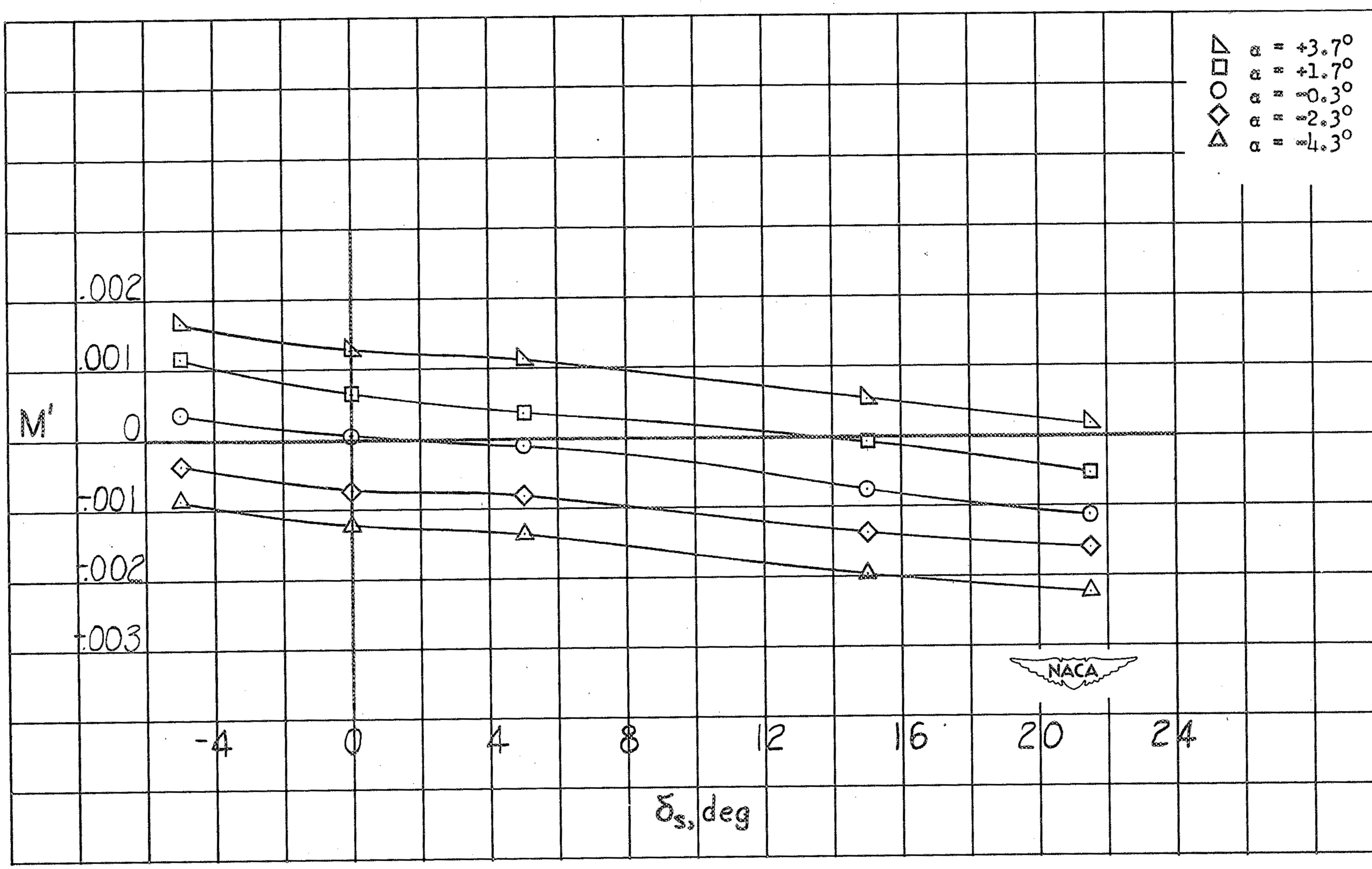

(b) Scheme-2 tail with 202-square-foot diving plane.

Figure 10.- Continued.

CONFIDENTIAL

NACA SL50E09a

CONFIDENTIAL

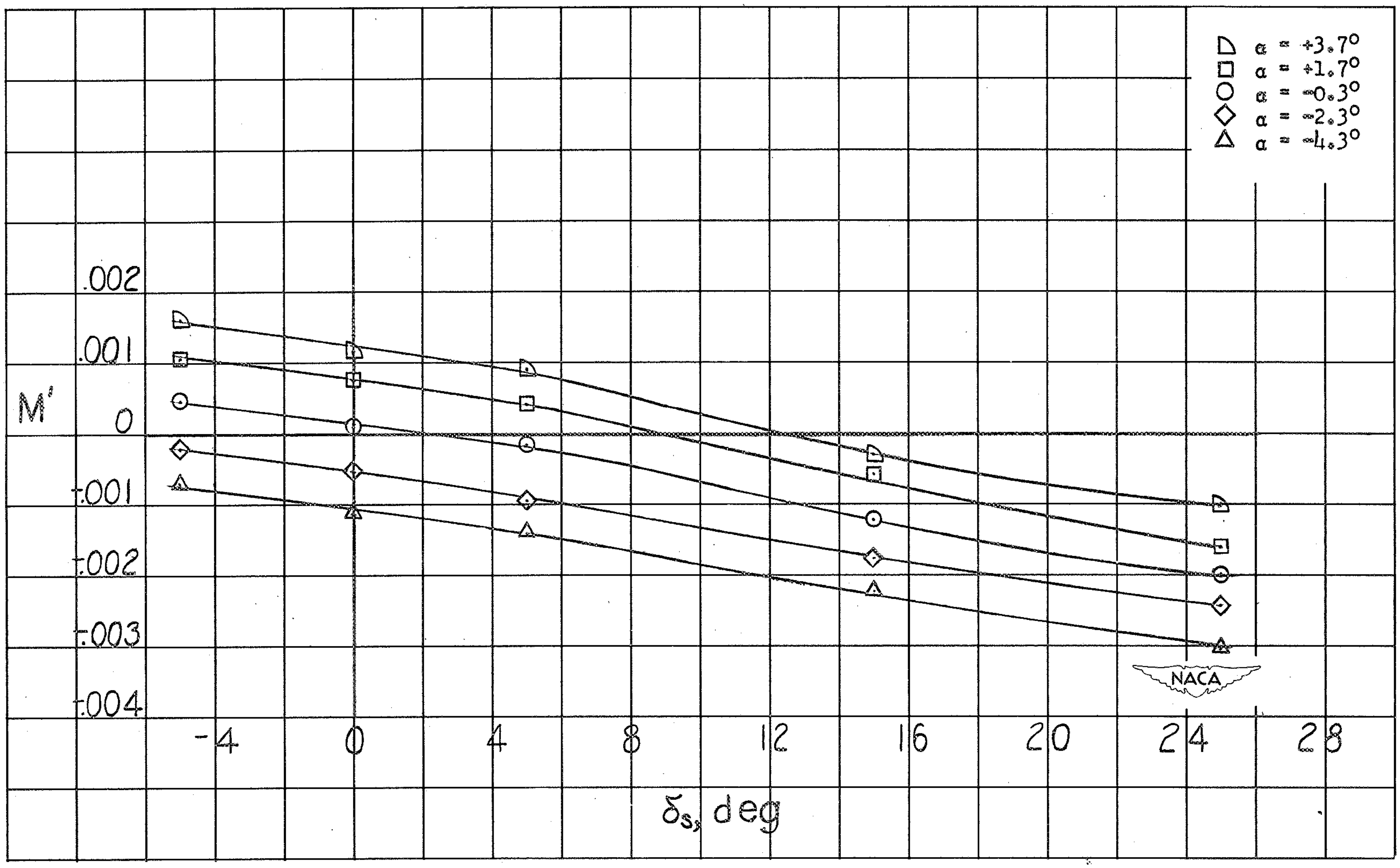

(c) Forward-located tail configuration.

Figure 10.- Concluded.

CONFIDENTIAL

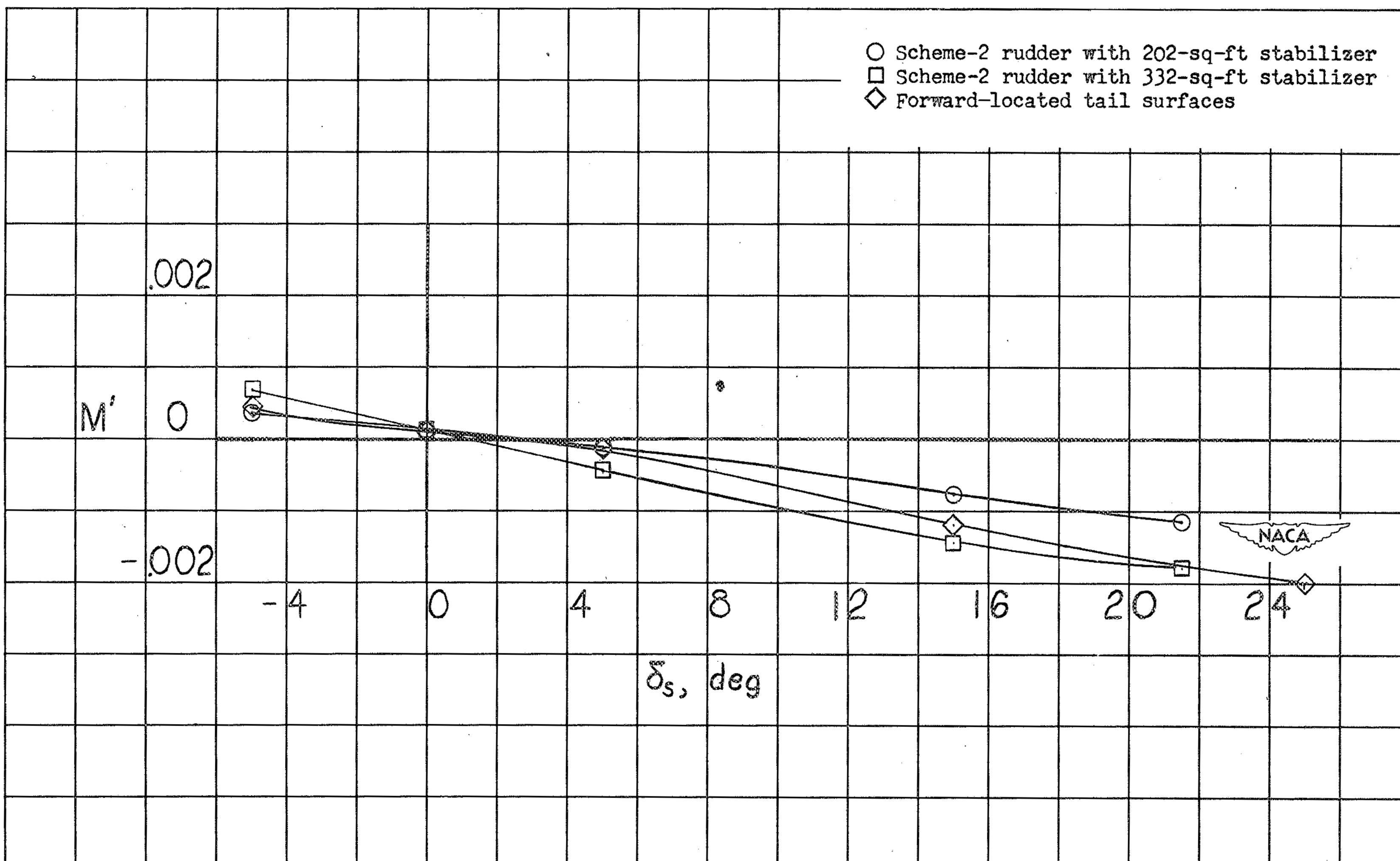

Figure 11.- Pitching-moment coefficient variation with diving-plane deflection for three tail configurations. $\alpha = -0.3^{\circ}$; $\psi = 0^{\circ}$; $\delta_r = 0^{\circ}$.

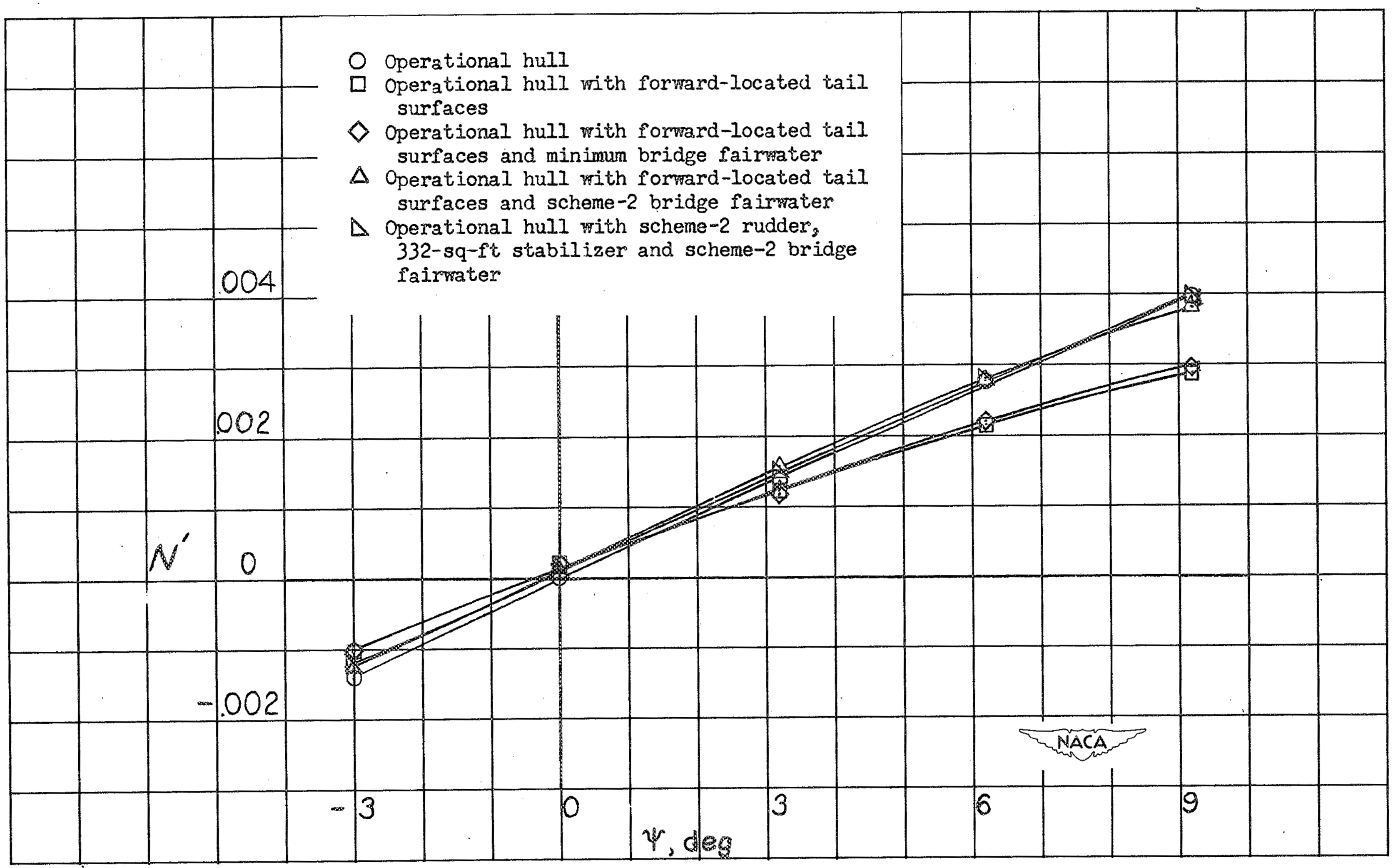

(a) Yawing-moment coefficient, N'.

Figure 12.- Variation of N', K', M', and Y' with yaw for five model configurations. $\alpha = -0.3^{\circ}$; $\delta_r = 0^{\circ}$; $\delta_s = 0^{\circ}$.

316112

NACA SL50E09a

CONFIDENTIAL

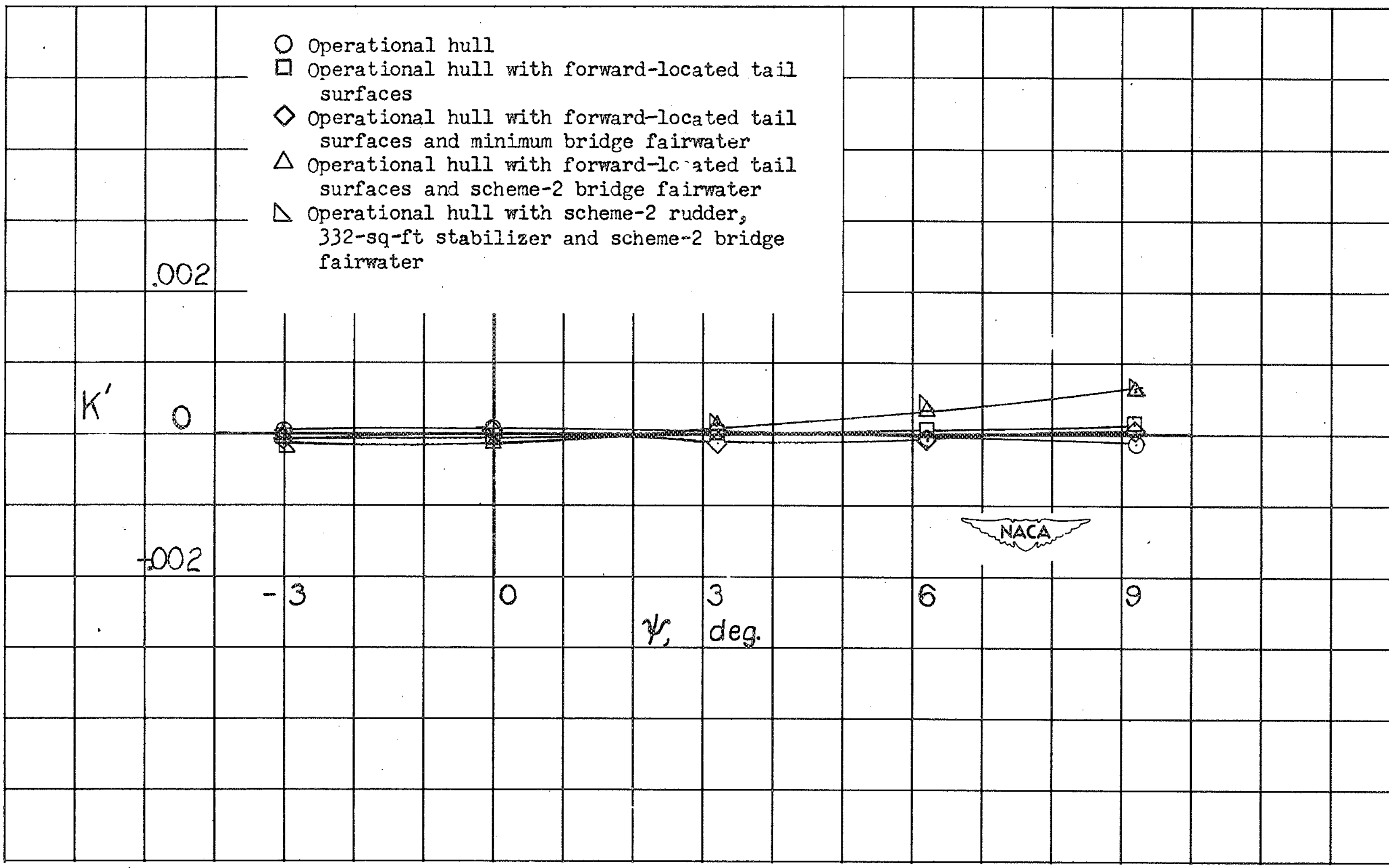

(b) Rolling-moment coefficient, K'.

Figure 12.- Continued.

CONFIDENTIAL

CONFIDENTIAL

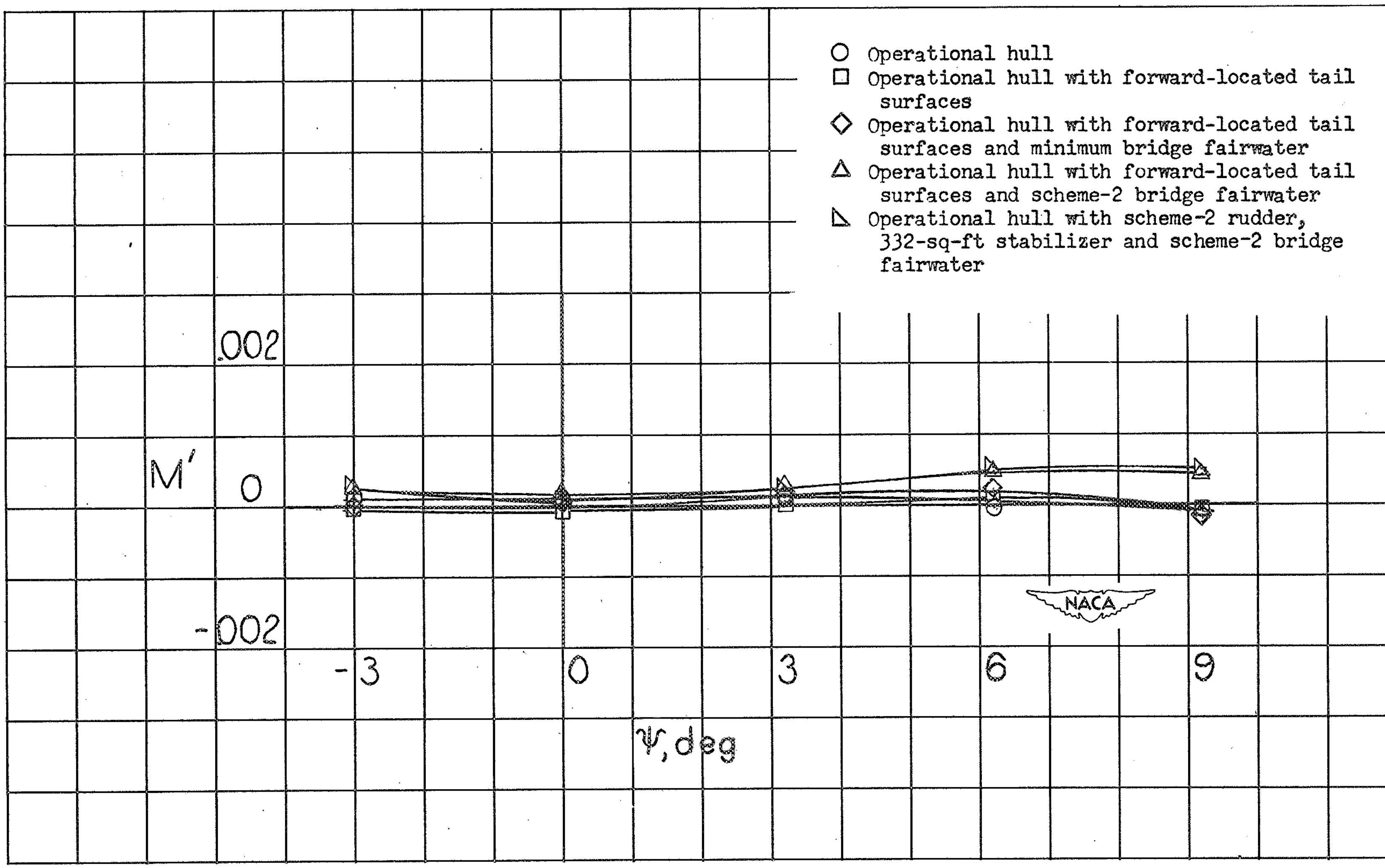

(c) Pitching-moment coefficient, M′.

Figure 12.- Continued.

CONFIDENTIAL

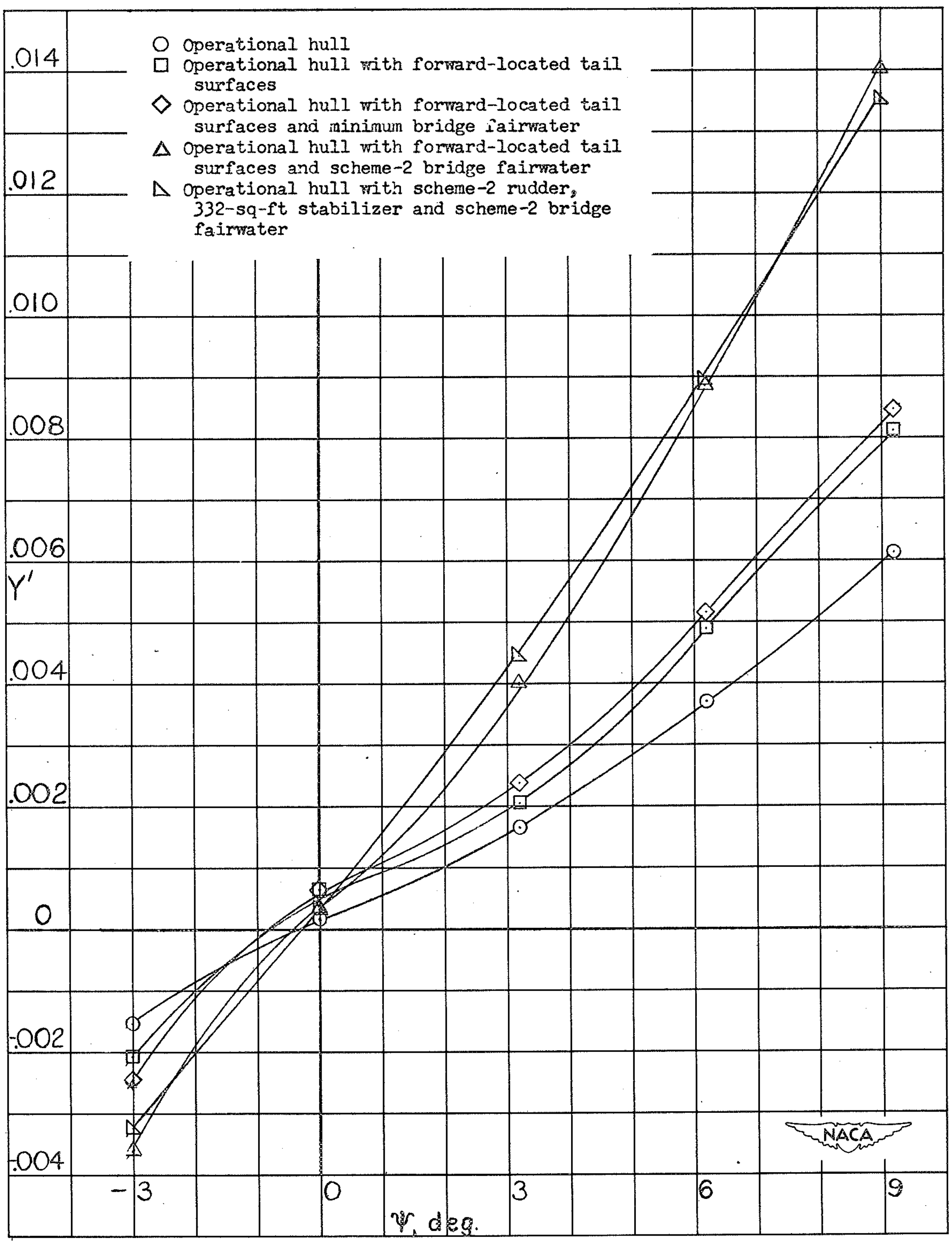

(d) Lateral-force coefficient, Y'.

Figure 12.- Concluded.

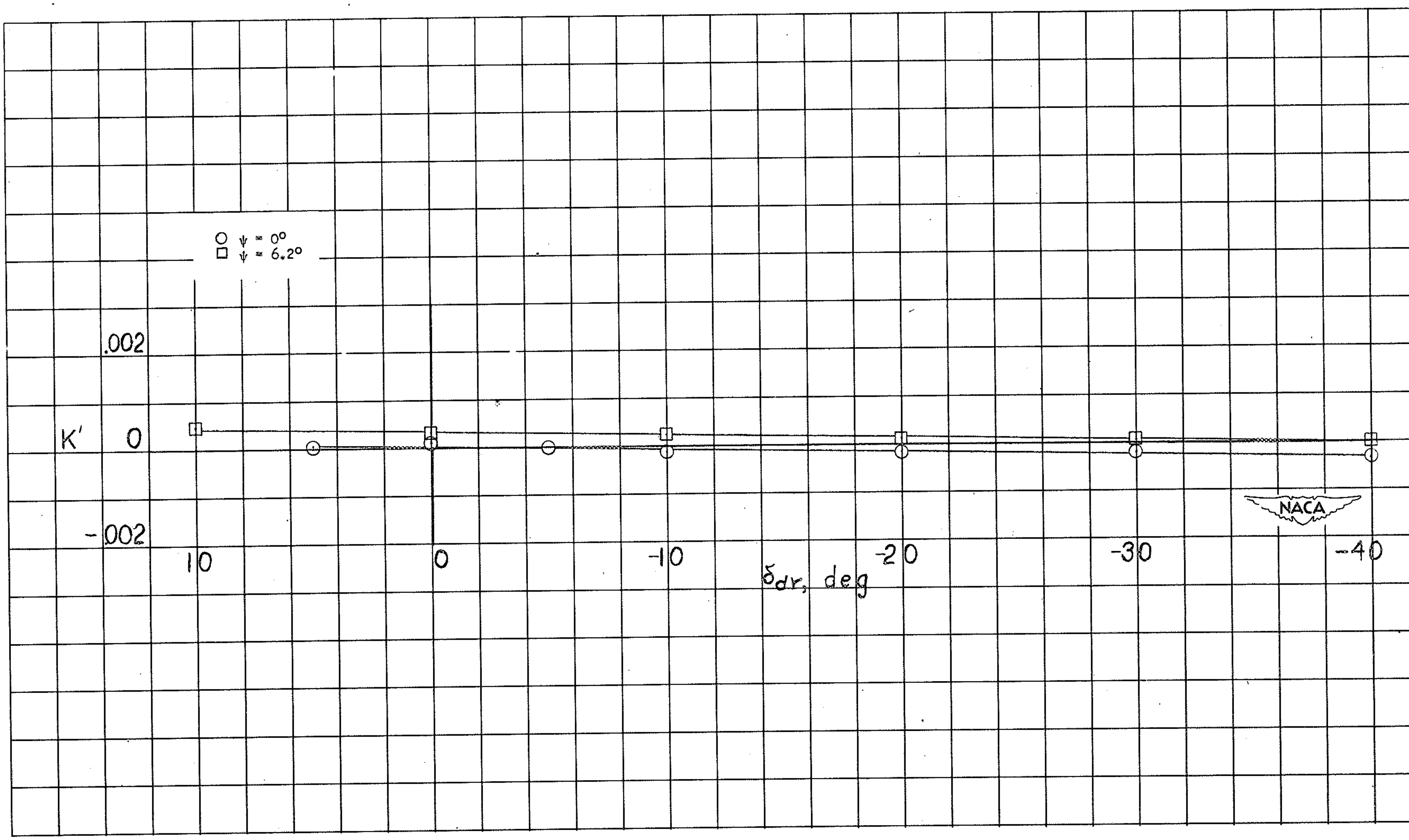

Figure 13.- Variation of rolling-moment coefficient with deflection of bridge fairwater dorsal rudder. $\alpha = -0.3^{\circ}$; $\delta_r = 0^{\circ}$; $\delta_s = 0^{\circ}$.

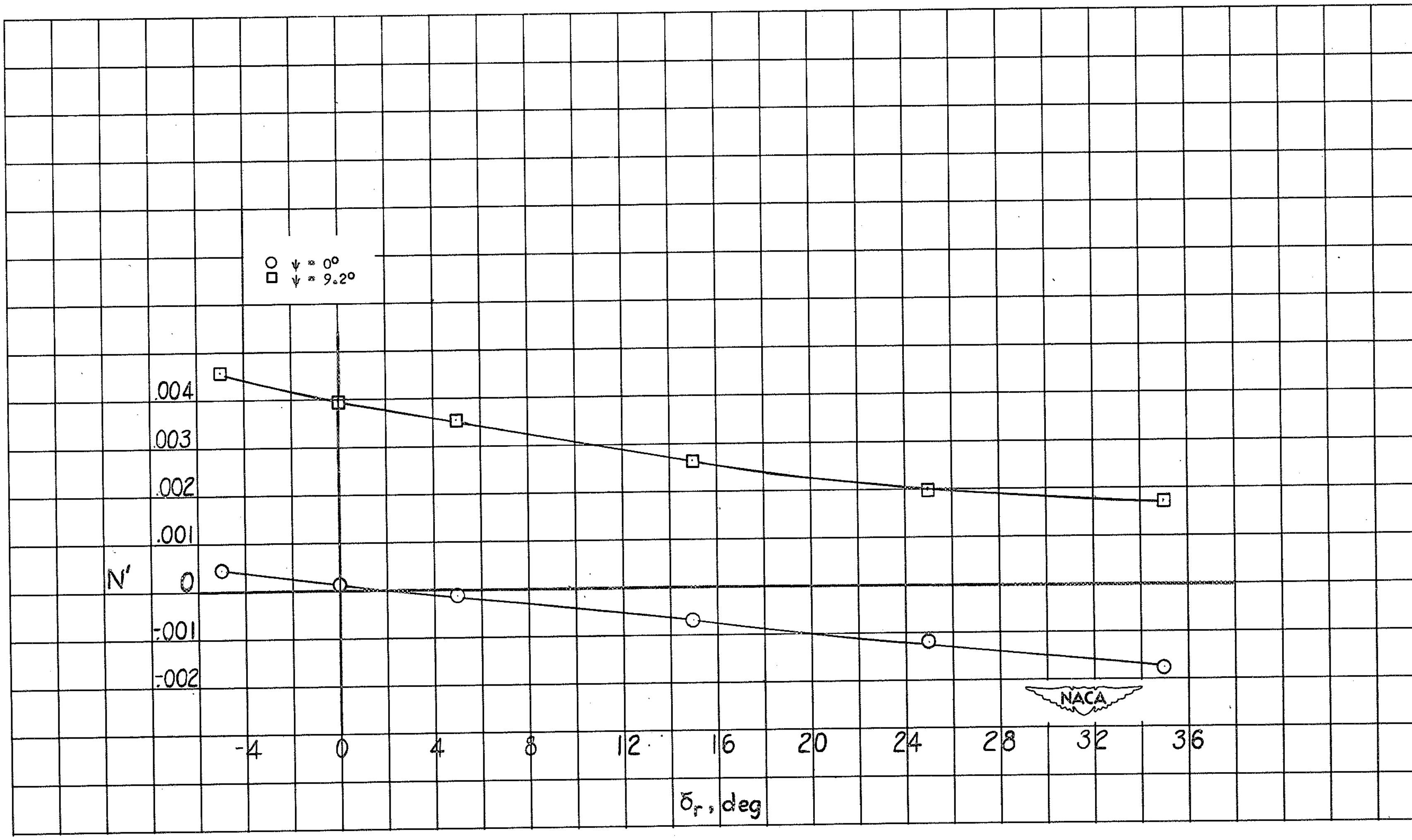

(a) Scheme-2 fin and rudder with 332-square-foot diving plane installed.

Figure 14.- Variation of yawing-moment coefficient with rudder deflection for two tail configurations. $\alpha = -0.3^{\circ}$; $\delta_s = 0^{\circ}$.

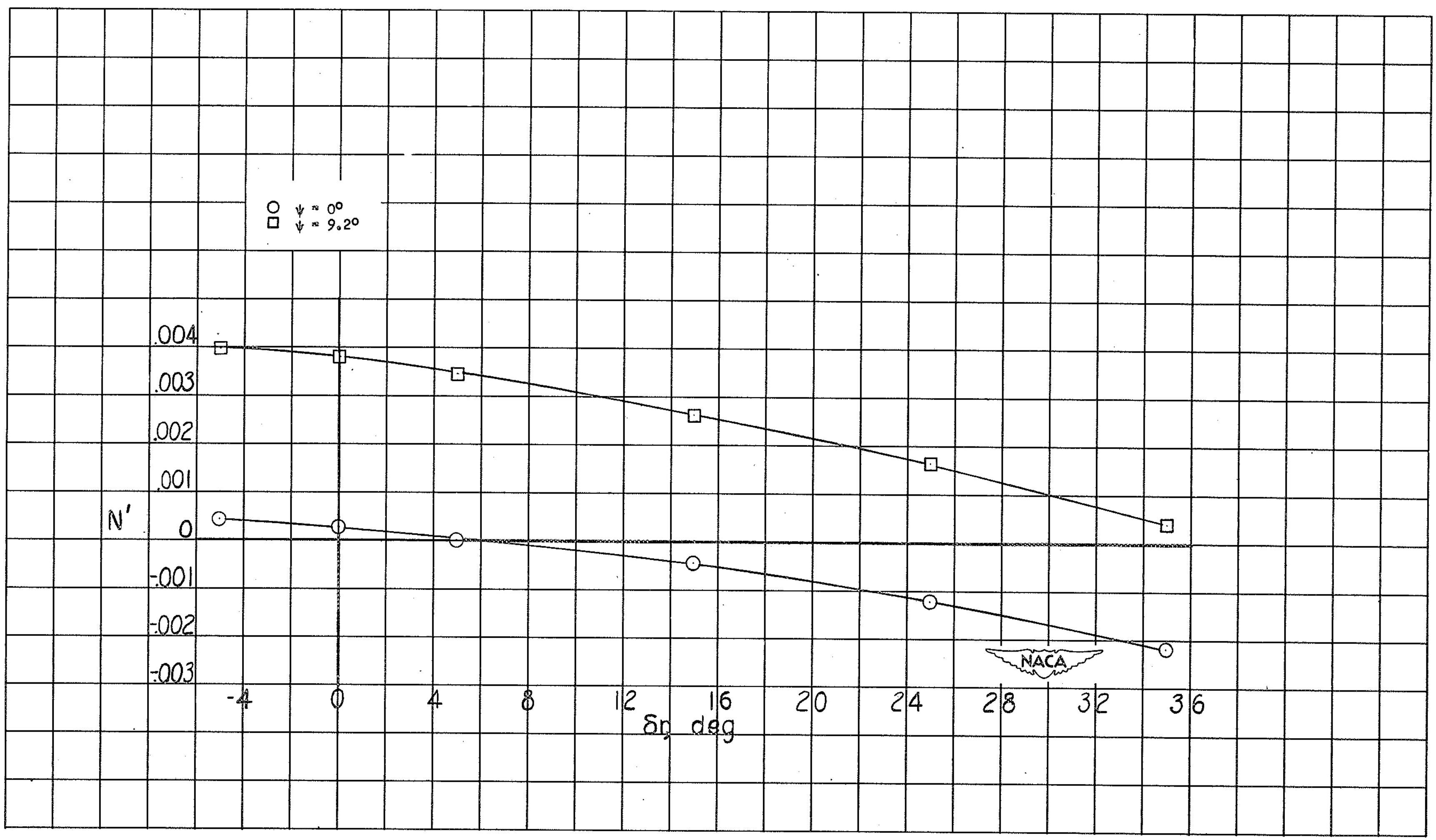

(b) Forward-located tail surfaces installed.

Figure 14.- Concluded.

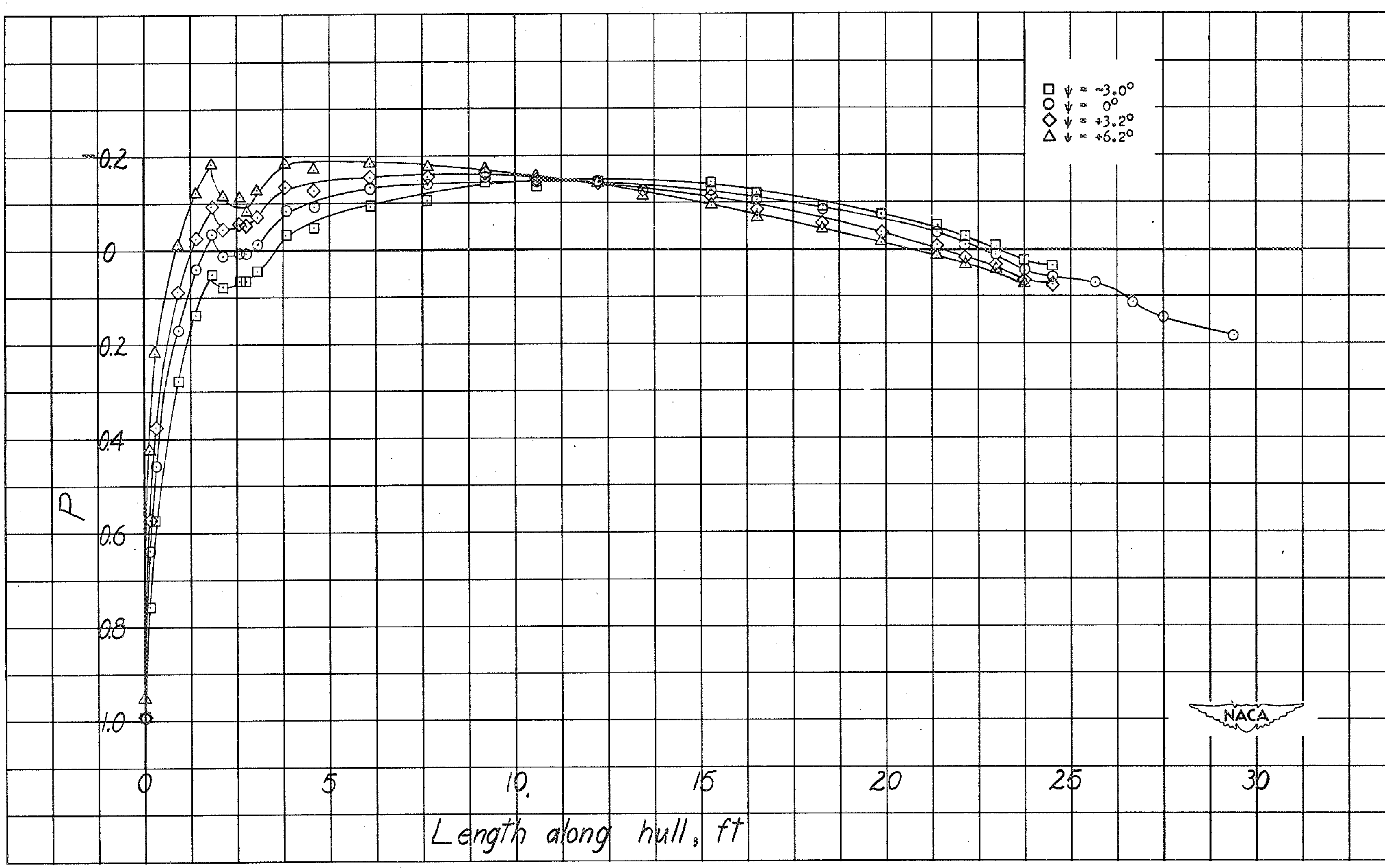

Figure 15.- Effect of yaw on hull pressure distribution along the starboard side of hull. $\alpha = -0.3^{\circ}$.

CONFIDENTIAL

NACA SL50E09a

CONFIDENTIAL

CONFIDENTIAL

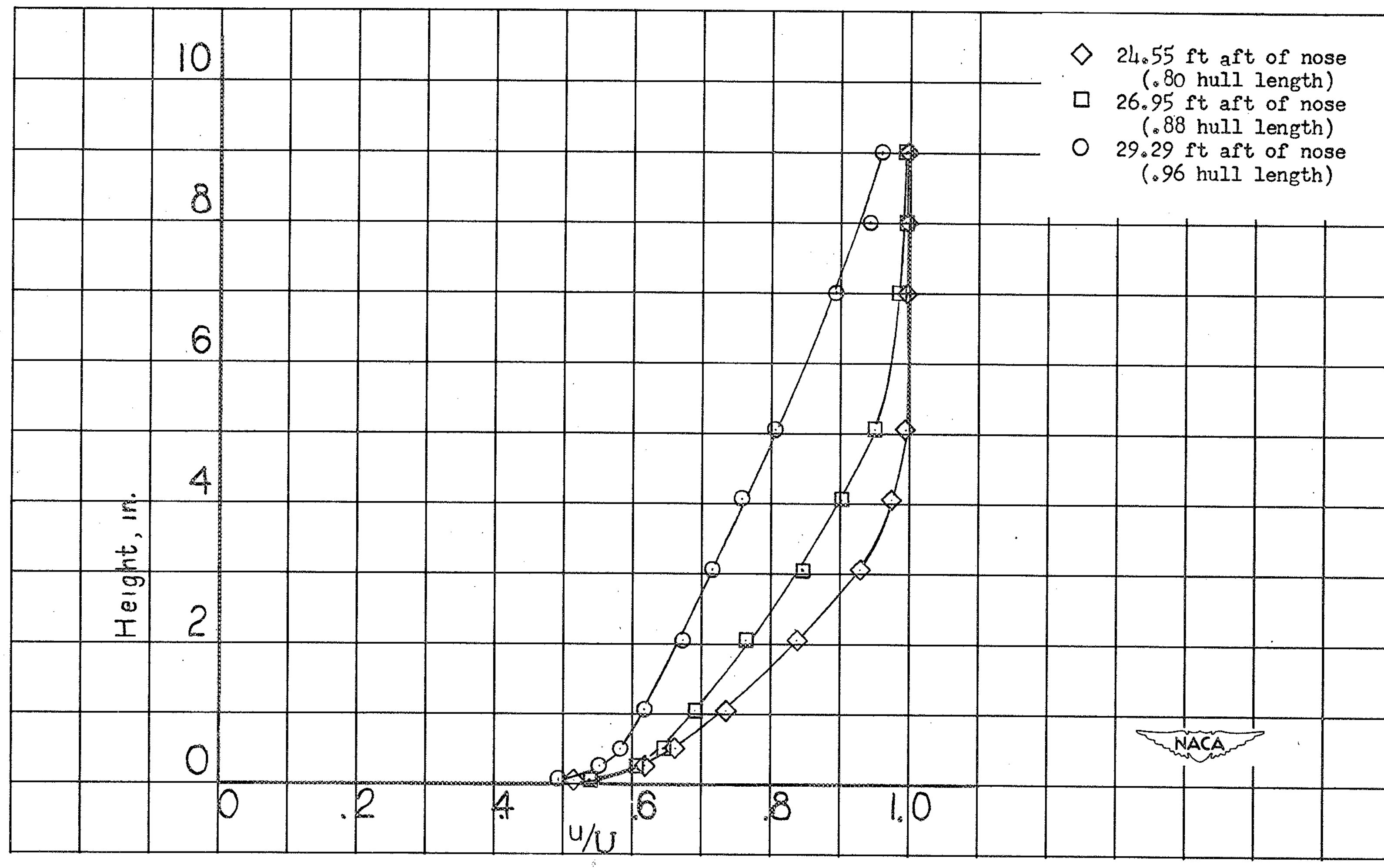

(a) Effect of longitudinal position. $\alpha = -0.3^{\circ}$.

Figure 16.- Velocity profiles in the boundary layer along the top center line of the hull. $\psi = 0^{\circ}$.

CONFIDENTIAL

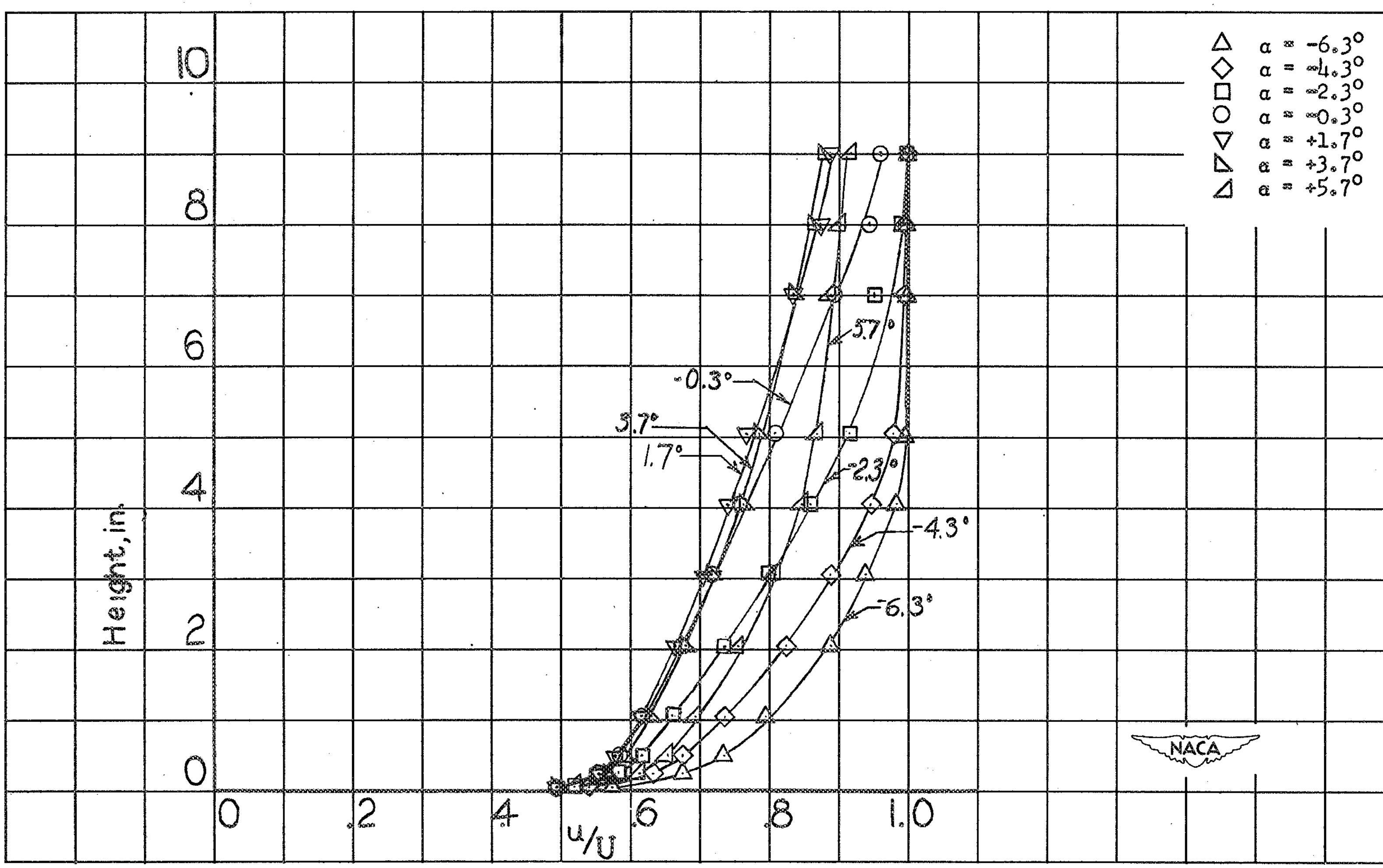

(b) Effect of angle of attack. Position, 0.96l.

Figure 16.- Continued.

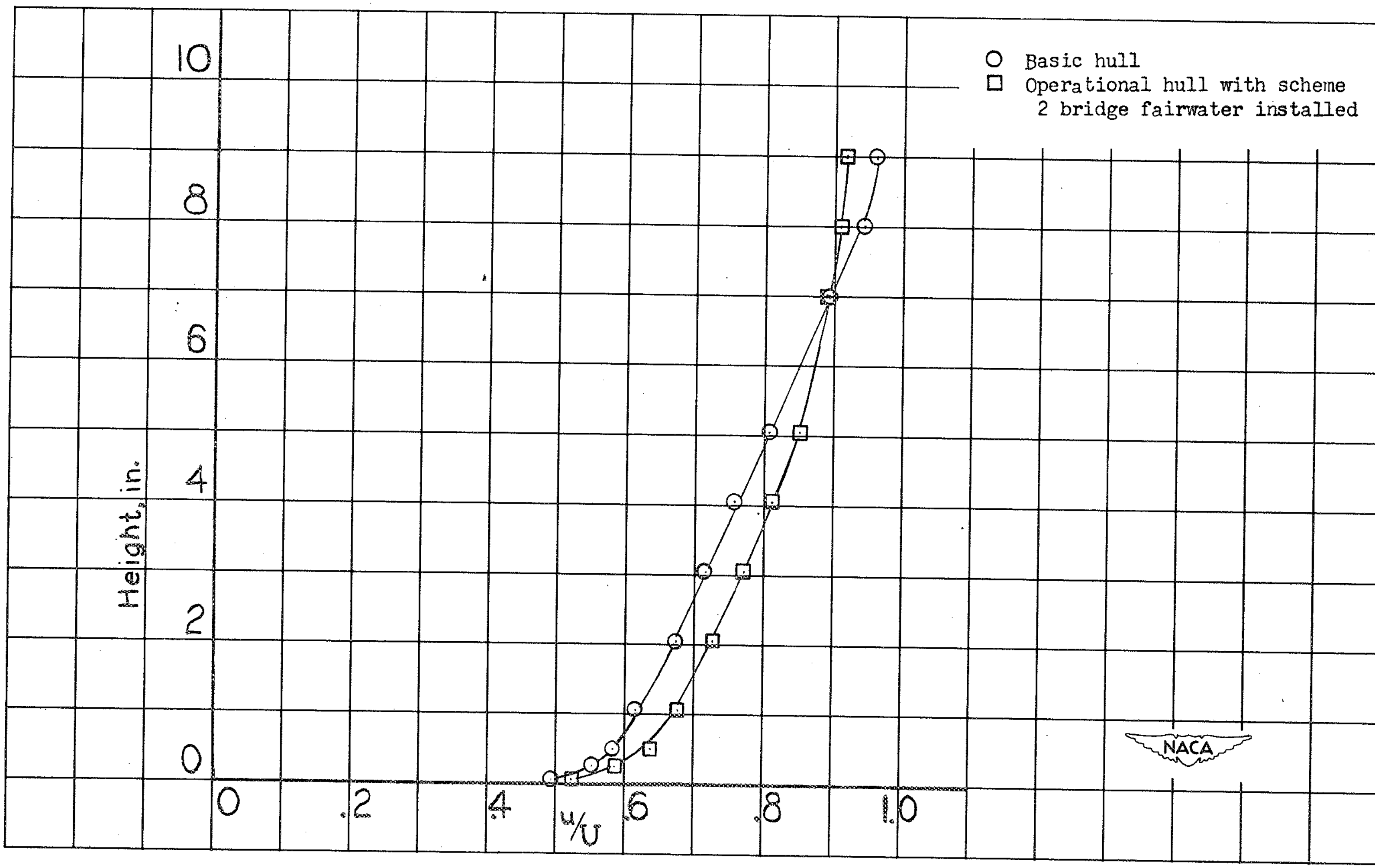

(c) Effect of hull condition. $\alpha = -0.3^{\circ}$; position, $0.96l$.

Figure 16.- Concluded.

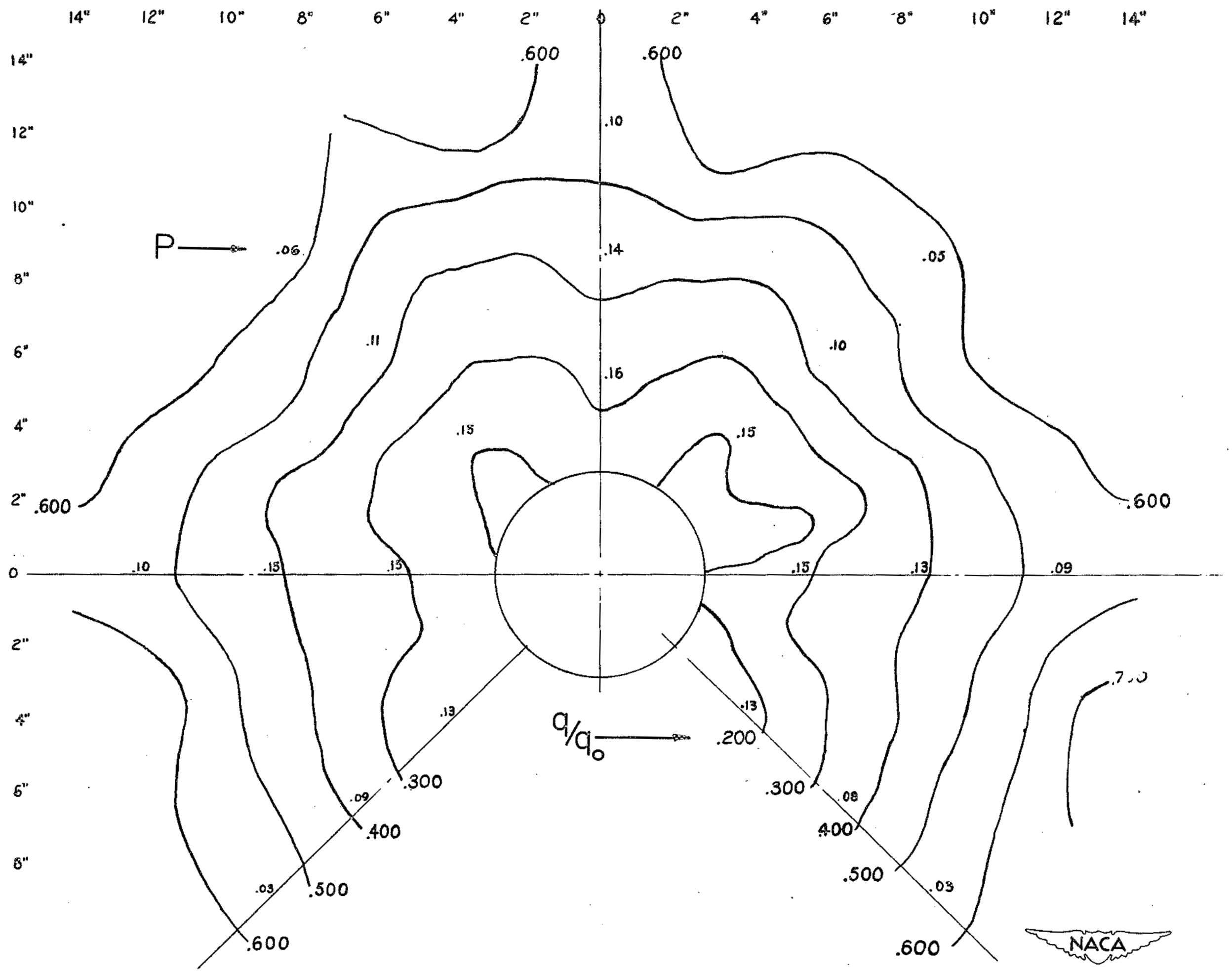

(a) In the plane of propeller.

Figure 17.- Variation of local dynamic pressure ratios in the region of the propeller. Complete scheme-2 configuration with 332-square-foot diving plane. Propeller removed. $\alpha = -0.3^{\circ}$; $\psi = 0^{\circ}$.

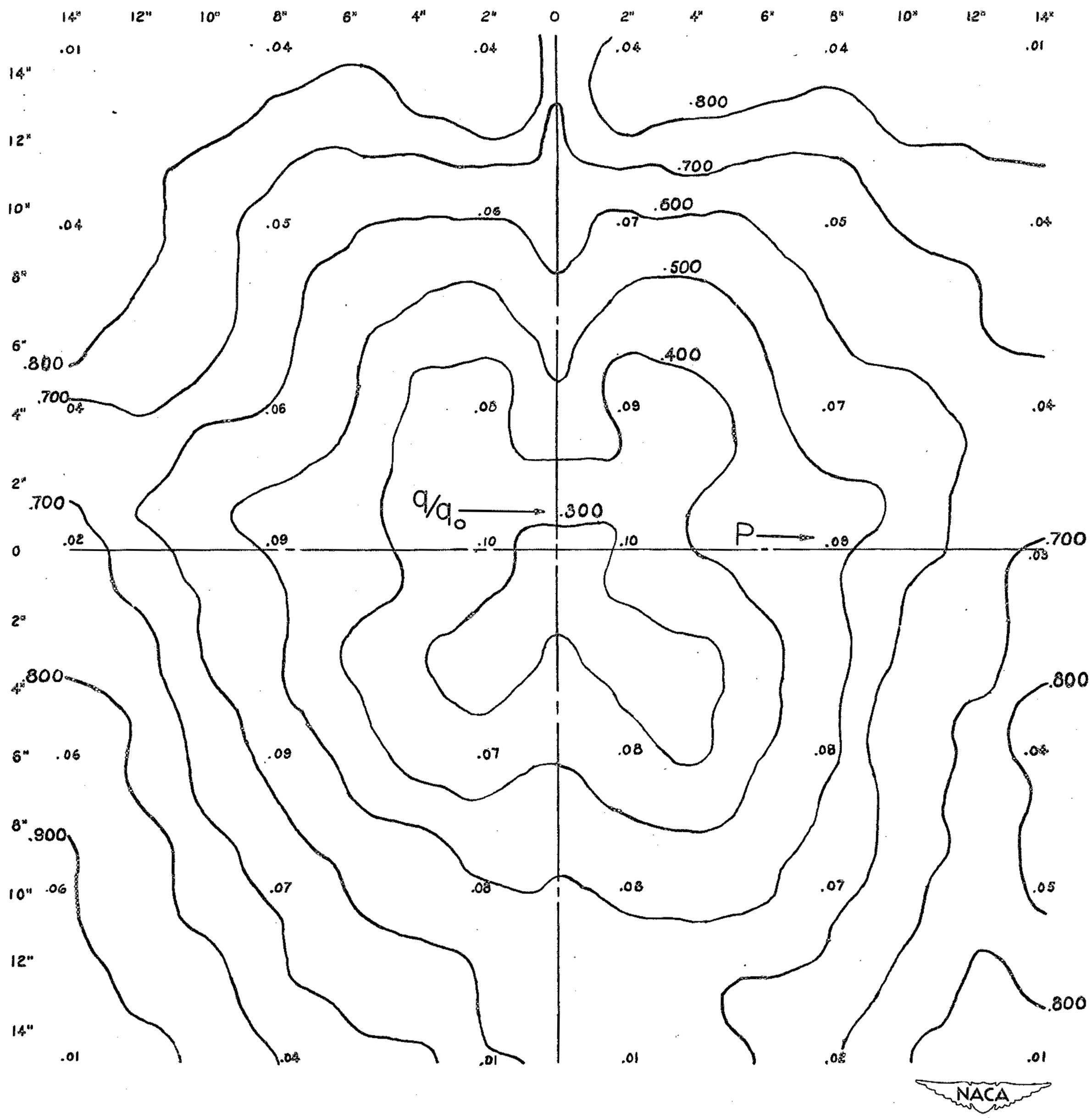

(b) Nine inches aft of propeller.

Figure 17.- Concluded.

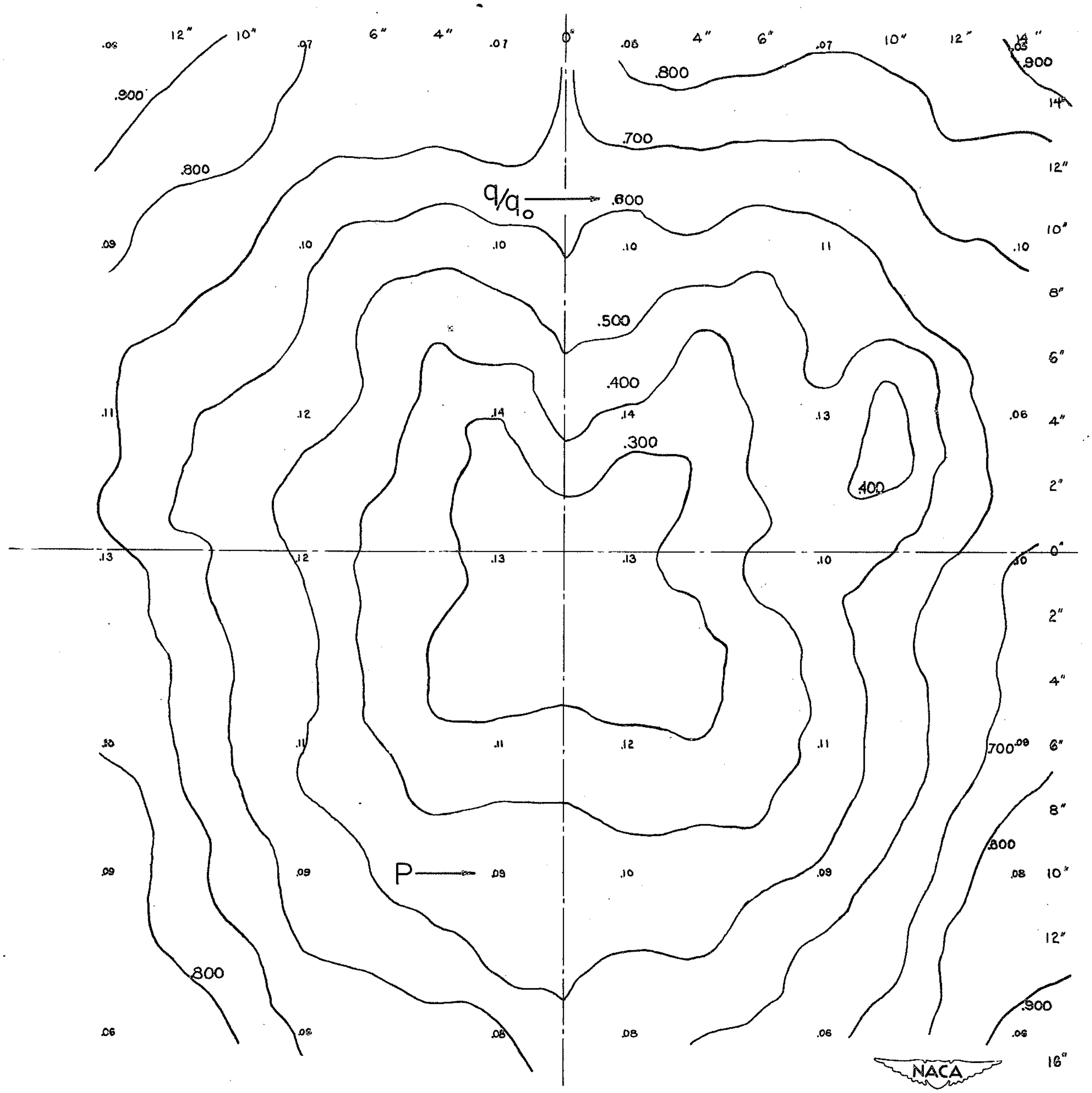

Figure 18.- Variation of local dynamic-pressure ratios in a plane 9 inches aft of the propeller. Complete scheme-2 configuration with forward-located tails. Propeller removed. $\alpha = -0.3^{\circ}$; $\psi = 0^{\circ}$.